Automatica, Vol. 41 (2005), pp. 439-457.

Relations between uncertainty structures in identification for robust control ⋆

Sippe G. Douma [a], Paul M.J. Van den Hof [a]

[a] *Delft Center for Systems and Control, Delft University of Technology, Mekelweg 2, 2628 CD Delft, The Netherlands*

Abstract

Various techniques of system identification exist providing for a nominal model and an uncertainty bound. An important question is what the implications are for the particular choice of the structure in which the uncertainty is described when dealing with robust stability/performance analysis of a given controller and when dealing with robust synthesis. It is shown that an amplitude-bounded (circular) uncertainty set can equivalently be described in terms of an additive, Youla parameter and ν-gap uncertainty. As a result, the choice of structure does not matter provided that the identification methods deliver optimal uncertainty sets rather than an uncertainty bound around a prefixed nominal model. Frequency dependent closed-loop performance functions based on the uncertainty sets are again bounded by circles in the frequency domain, allowing for analytical expressions for worst-case performance and for the evaluation of the consequences of uncertainty for robust design. The results can be used to tune optimal experimental conditions in view of robust control design and in the further development of experiment-based robust control design methods.

Key words: Identification for control; robust stability; gap metric; Youla parametrization; model uncertainty; robust control; system identification

1 Introduction

In identification for (robust) control several stages can be recognized in the research results that have been obtained over the last decade. In the pre-1990's the certainty equivalence principle was dominant: an exact plant model is identified that is to be used in model-based (nominal) control. In the early nineties the focus was on identifying approximate nominal models for control (see e.g. [13,31]), identifying models that focus on the control-relevant aspects of the plant. Around the same time, model uncertainty sets were constructed from measurement data, first in a worst-case deterministic setting (for an overview see [5]), but also in a probabilistic ([16]) and combined deterministic-probabilistic framework ([9,18]). In identification for control, these uncertainty sets are typically used to verify the robustness properties (robust stability and robust performance) of a controller designed on the basis of a nominal model only, i.e. nominal design plus robustness analysis. For the "classical" prediction error identification methods, particular tools for robustness analysis have been developed ([2]) as well as for model and controller validation ([14]). Additionally a large number of uncertainty descriptions is available from robust control theory, as e.g. a (H_∞)-norm-bounded additive or multiplicative uncertainty on the plant model, a norm-bounded uncertainty on a closed-loop plant representation (e.g. its dual Youla parameter), uncertainties bounded in the gap or ν-gap metric, and real parametric uncertainties, see e.g. [34,35,29]. In the next phase of research it is recognized that for an optimal robust controller, it is not only necessary that the nominal model is control-relevant, but also that the model uncertainty is smallest in the control-relevant (frequency) region. This latter property is required for the designed robust controller to achieve a satisfactory level of performance. Identification for control methods that include a robust design (rather than a nominal design with robustness analysis) were considered in [7,6]. This includes the iterative identification of control-relevant model uncertainty sets.

An excellent overview of this development, including aspects of experiment design, is given in [21].

Both in the robustness analysis and in the robust synthesis problems, the choice for an appropriate model uncertainty structure is important. From an identification experiment the measurement data is typically mapped into an uncertainty set that is represented in a particular structure, as e.g. parametri-

⋆ Preliminary versions of this paper were presented at the 41th IEEE Conf. Decision and Control, December 2002, Las Vegas, NA, and at the 13th IFAC Symp. System Identification, August 2003, Rotterdam, The Netherlands. Corresponding author Paul Van den Hof. Tel. +31 (0)15-27 84509. Fax +31 (0)15-27 86679.

Email address: p.m.j.vandenhof@dcsc.tudelft.nl (Paul M.J. Van den Hof).

cally structured (ellipsoidal) uncertainty, norm-bounded additive, non-parametric (boxed, ellipsoidal) additive in the frequency domain [25,16,18,9].
Amongst such a variety of possible uncertainty structures a relevant question is what the implications are of a particular choice of structure for the identification for robust control problem. An ultimate question to be answered would be what is, for a given purpose (robust stability/performance analysis or synthesis), the best model uncertainty structure in which to identify the model set (nominal model and uncertainty bound). And consequently, what would be the best experiment allowing for minimization of the uncertainty.
In this paper the former problem will be taken at hand. While extensive literature exists dealing with characteristics of each uncertainty structure, answering the posed question requires a thorough comparison and a bridging of the gap between identification and robust control that goes beyond the present state of the art. A first attempt with limited scope only directed towards robust stability issues was made in [12]. Computational tools for calculating robust performance over uncertainty sets are available for many structures [35,34]. Here we will focus in particular on analytical expressions.
This paper is intended to highlight aspects in which the various uncertainty structures differ in their consequences for robust analysis and design and in their potentials to be determined on the basis of realistic experimental data. In the next section the uncertainty structures and the performance measure are specified. The third section explores the link between the uncertainty structures and their behaviour under a linear fractional transformation. In the last three sections the uncertainty (structure) is analyzed with respect to, respectively, robust stability and robust performance (analysis/synthesis).

2 Framework

We consider single-input-single-output linear time-invariant finite dimensional systems $G(s)$ and controllers $C(s)$. Coprime factorizations of plants and controllers are defined as $G(s) = N(s)D^{-1}(s)$ and $C(s) = N_c(s)D_c^{-1}(s)$ where $N(s), D(s), N_c, D_c \in \mathbb{R}H_\infty$ satisfy the usual conditions [33]. The factorizations are normalized, denoted by $\overline{(\cdot)}$, if they additionally satisfy $\bar{N}(s)^*\bar{N}(s) + \bar{D}(s)^*\bar{D}(s) = 1$, where $(\cdot)^*$ denotes complex conjugate transpose. This paper considers three model sets based on a specific uncertainty structure:

Additive uncertainty

$$G_a(G_x, W_a) := \{G_\Delta(s) \mid G_\Delta(s) = G_x(s) + \Delta_a(s)\ , \quad |\Delta_a(i\omega)| \le |W_a(i\omega)| \quad \forall \omega \in \mathbb{R}\}, \tag{1}$$

with $G_x(s)$ a nominal model and $W_a(s)$ a weighting function.

Youla-uncertainty

$$G_Y(G_x, C, Q, Q_c, W_Y) := \left\{ G_\Delta(s) \mid G_\Delta(s) = \frac{\bar{N}_x(s) + \bar{D}_c(s)\Delta_G(s)}{\bar{D}_x(s) - \bar{N}_c(s)\Delta_G(s)}\ , \ \left|Q_c^{-1}(i\omega)\Delta_G(i\omega)Q(i\omega)\right| \le |W_Y(i\omega)| \quad \forall \omega \in \mathbb{R} \right\}. \tag{2}$$

with $G_x(s) = \bar{N}_x(s)\bar{D}_x^{-1}(s)$ a nominal model, $C(s) = \bar{N}_c(s)\bar{D}_c^{-1}(s)$ a present controller and $Q(s)$,$Q_c(s)$ stable and stably invertible weighting functions reflecting the freedom in choosing the coprime factorizations of $G_x(s)$ and $C(s)$ [33]. An additional weighting can be provided by $W_Y(s)$. The Youla parameter $\Delta_G(s)$ is uniquely determined by $\Delta_G(s) = \bar{D}_c^{-1}(s)(1 + G_\Delta(s)C(s))^{-1}\ (G_\Delta(s) - G_x(s))\bar{D}_x(s)$.

ν-*gap uncertainty* [34]

$$G_\nu(G_x, W_\nu) := \{G_\Delta(s) \mid \kappa(G_\Delta(i\omega), G_x(i\omega)) \le |W_\nu(i\omega)| \quad \forall \omega \in \mathbb{R}\}, \tag{3}$$

with $\kappa(G_\Delta, G_x)$ the chordal distance between a plant $G_\Delta(s) = \bar{N}_\Delta(s)\bar{D}_\Delta^{-1}(s)$ and the nominal model $G_x(s) = \bar{N}_x(s)\bar{D}_x^{-1}(s)$, defined by

$$\kappa(G_\Delta(i\omega), G_x(i\omega)) := |\bar{N}_x(i\omega)\bar{D}_\Delta(i\omega) - \bar{D}_x(i\omega)\bar{N}_\Delta(i\omega)| = \frac{|G_x(i\omega) - G_\Delta(i\omega)|}{\sqrt{\left(1 + |G_\Delta(i\omega)|^2\right)\left(1 + |G_x(i\omega)|^2\right)}}.$$

Note that at this point pole/zero conditions are not yet imposed on $G_\Delta(s), G_x(s), \Delta(s), P(s)$ or $W(s)$ as required when studying robust stability conditions. The focus lies here with the properties of the frequency responses of the sets. In section 4 the particular stability conditions will be discussed.
We consider a frequency-dependent control performance measure:

$$J(G_\Delta, C, V, W) := \bar{\sigma}(V(i\omega)T(G_\Delta(i\omega), C(i\omega))W(i\omega)), \tag{4}$$

with $\bar{\sigma}$ the maximum singular value and

$$T(G_\Delta, C) := \begin{bmatrix} G_\Delta \\ 1 \end{bmatrix} (1 + G_\Delta C)^{-1} \begin{bmatrix} C & 1 \end{bmatrix}. \tag{5}$$

The weighting matrices V and W are diagonal. These diagonal weighting functions allow for a large range of performance specifications, such as weighted sensitivity or complementary sensitivity function [35], loop-shaped performance [26,34] and more general versions [8] .

Remark 1 *From here onwards the arguments s and $i\omega$ are omitted to include both an evaluation in terms of transfer functions (e.g. $G(s)$) with frequency responses over the whole frequency axis, and an evaluation over a frequency grid with, e.g. $G(i\omega_k) \in \mathbb{C}$, $\omega_k \in \Omega \in \mathbb{R}$. Throughout the paper*

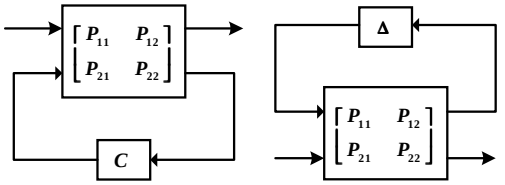

Fig. 1. Lower (a. left) and upper (b. right) linear fractional transformations in a control loop of a model with uncertainty.

results will be formulated in terms of frequency responses. However, all results are such that they hold true for transfer functions. Substitution of $|X|^2$ *by* $X(s)X^*(s)$ *and interpreting* $\sqrt{|X|^2}$ *as the spectral root of* $X^*(s)X(s)$ *will allow for a formulation in terms of (rational) systems.*

A convenient way of dealing with model uncertainty and closed-loop performance functions is in terms of upper and lower linear fractional transformations (Fig. 1). The mapping of the open-loop transfer functions G_Δ to the closed-loop performance functions in (5) can be described with a lower linear fractional transformation (LFT) $F_\ell(P,C) := P_{11} + P_{12}C(1+P_{22}C)^{-1}P_{21}$. This is indicated in Figure 1(a). Similarly, the three uncertainty sets above can be described in terms of an upper LFT (see Figure 1(b)): $F_u(P,C) := P_{22} + P_{21}\Delta(1+P_{11}\Delta)^{-1}P_{12}$, a fact that is shown in the subsequent sections. As a result, for the discussion in this paper it will be essential to specify the consequences of LFT mappings when applied to uncertainty sets. This will be the topic of the next section.

3 Effect of linear fractional transformations

3.1 Mapping of circles

It is well known that a linear fractional transformation (Möbius transformation) maps circles into circles. Here we will recall this result in an explicit formulation (see e.g. [10]). Such a formulation allows for much insight when comparing uncertainty structures and assessing their influence on performance.

Proposition 1 *A set of frequency responses described by the (SISO) LFT*

$$F(P,\Delta) = P_{22} + P_{21}\Delta(1+P_{11}\Delta)^{-1}P_{12}\ , \quad \textit{with}\ \left|W^{-1}\Delta\right| \le 1 \tag{6}$$

and a one-dimensional uncertainty block Δ*, can at each frequency be described in an additive structure as*

$$F(P,\Delta) = F_{centre} + \Delta_a, \quad \left|W_a^{-1}\Delta_a\right| \le 1,$$

with

$$F_{centre} = P_{22} + \frac{-P_{21}P_{12}P_{11}^*|W|^2}{1-|P_{11}W|^2}, \qquad W_a = \frac{P_{21}P_{12}}{1-|P_{11}W|^2}W$$

provided that $|P_{11}W| < 1$*. Whenever* $|P_{11}W| > 1$*, the frequency responses of the set* $F(P,\Delta)$ *lie in the area outside the circle* $F_{centre} + \Delta_a$*,* $\left|W_a^{-1}\Delta_a\right| = 1$*.*

Proof Consider the simple linear fractional transformation $Z = \dfrac{1}{1+\Delta}, |\Delta| \le |W|$. Since $\Delta = \frac{1-Z}{Z}$ it holds that

$$|1-Z|^2 \le |W|^2|Z|^2$$

With $|1-Z|^2 = (1-Z)(1-Z)^*$, this reads

$$|Z|^2\left(1-|W|^2\right) - Z - Z^* \le -1$$

which with completion of the squares results in

$$\left|Z - \frac{1}{1-|W|^2}\right|^2 \le \frac{|W|^2}{\left(1-|W|^2\right)^2}$$

where the inequality sign should be reversed in case $\left(1-|W|^2\right) < 0$. Therefore, it holds that

$$Z = \frac{1}{1-|W|^2} + \Delta_Z, \quad \text{with } |\Delta_Z| \le \frac{|W|}{\left(1-|W|^2\right)}. \tag{7}$$

As the LFT $F(P,\Delta)$ of expression (6) can be written as,

$$F(P,\Delta) = P_{22} + \frac{P_{21}P_{12}}{P_{11}}\left(1 - \frac{1}{(1+P_{11}\Delta)}\right),$$

Proposition 1 is seen to hold by shifting and scaling with respect to the result in expression (7). □

The proposition shows that a circular region in the frequency domain is again mapped into a circle. However, the original centre (P_{22}) is not the new centre unless the linear fractional transformation happens to be affine ($P_{11} = 0$). Further, the radius $|W_a|$ is easily shown to increase whenever $|W|$ is increasing as long as $|P_{11}W| < 1$. In this case the interior of the circle defined by $|W|$ is mapped to the interior of the circle defined by F_{centre} and $|W_a|$. The radius $|W_a|$ decreases with $|W|$ whenever $|P_{11}W| > 1$, in which case the interior of the first set is mapped to the exterior of the latter one.

3.2 Mapping of non-circular bounds and probability density functions

Uncertainty regions resulting from system identification are not necessarily circular. Techniques based on statistical considerations as [9,18,16,25] usually provide for ellipsoidal or boxed uncertainty regions at each frequency, where the bound on the real and imaginary part is with respect to a certain probability level. Parameter bounding techniques

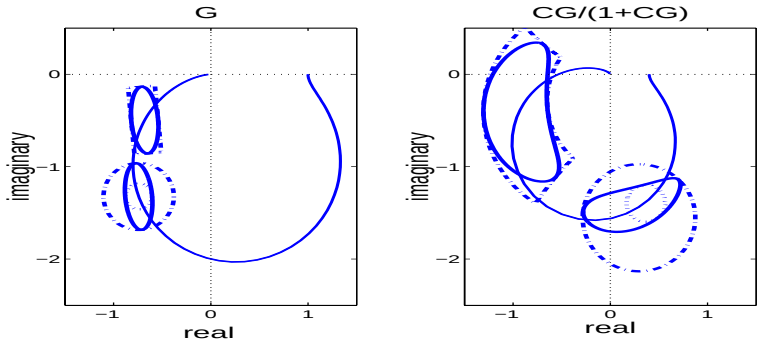

Fig. 2. Transformation of circular, ellipsoidal and boxed uncertainty bounds from plant model G (left) to closed-loop transfer model $CG/(1+CG)$ (right).

as in [27,17] induce polytopic uncertainty regions, while H_∞ identification procedures [5] essentially provide pointwise circular uncertainty regions in the frequency domain. A (SISO) LFT, being a conformal mapping, will map closed contours into closed contours and will leave angles locally intact. However, the mapping will in general not preserve shape, as depicted in Figure 2. In this figure it is illustrated that a circular uncertainty set for a plant G is mapped to a circular uncertainty set for the corresponding closed-loop plant $CG/(1+CG)$. Note however that concentric sets are not mapped to concentric sets, due to the fact that the centres of the sets are not maintained. The mapping of noncircular sets is not structure-preserving. Worst-case performance analysis and robust stability evaluation on such non-circular sets will require special, adapted procedures.

As indicated in [19] the transformation will change the structure of the probability distribution as well (see Figure 3). For example, when a closed-loop identified object $\hat{T} = \hat{G}C/(1+\hat{G}C)$ is used to obtain the open-loop plant model $\hat{G}$ by recalculation with the present controller C, i.e. $\hat{G} = \hat{T}/C(1-\hat{T})$, the statistical properties change drastically. An unbiased estimate of the closed-loop object does not imply an unbiased estimate of the recalculated open-loop plant. An important exception here is formed by all affine transformations $(P_{11} = 0)$. For these affine transformations the shape of the uncertainty sets remain invariant. This holds e.g. for the closed-loop function $T(G_\Delta, C)$ when applied to a Youla uncertainty set $G_Y(G_x, C, Q, Q_c, W_Y)$ with the present controller C. This is further elaborated in section 6.

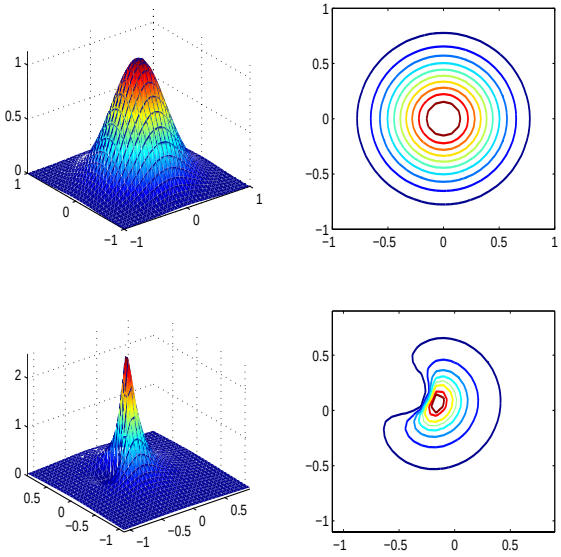

Fig. 3. Linear fractional transformation of a Gaussian distribution. A circular region (top right) associated with a p-% confidence region will be mapped to a circular region of again p-%. The latter, however, will not be the p-% confidence region with the smallest area under the new probability density function. The shape of the probability function changes drastically as can be seen from the contours of equal probability (bottom right).

4 Equivalence of uncertainty structures

The technical results of the previous section allow for a comparison between the additive, dual Youla and ν-gap uncertainty structures. Also the effect of conditions on the (unstable) poles and zeros of the plants in the uncertainty set will be discussed. The latter constraints are required when studying robust stability conditions.

4.1 Frequency responses in the uncertainty sets

All the uncertainty structures of Section 2 can equivalently be described by an additive structure in terms of their frequency domain properties. While this follows directly from Proposition 1 for e.g. the Youla parameter uncertainty structure, the ν-gap structure requires a separate proposition to show this fact. First Proposition 1 applied to the Youla parameter uncertainty structure is made explicit.

Corollary 1 *The set of frequency responses of all plants* $G_\Delta \in G_Y(G_x, C, Q, Q_c, W_Y)$ *(see (2)) is equivalently described as*

an additive uncertainty set $G_a(G_{centre}, W_a)$ (see (1)) with

$$G_{centre} = G_x\left(\frac{1}{1-|\bar{W}_Y|^2}\right) - C^{-1}\left(\frac{-|\bar{W}_Y|^2}{1-|\bar{W}_Y|^2}\right)$$
$$W_a = \frac{G_x + C^{-1}}{1-|\bar{W}_Y|^2}\bar{W}_Y,$$

where $\bar{W}_Y = \dfrac{\bar{N}_c Q_c}{\bar{D}_x Q} W_Y$.

Proof See appendix. □

Note that the centre of the Youla uncertainty set is given by a linear combination of the nominal model G_x and the negative inverse of the controller C used in the Youla parametrization.

The transformation of the ν-gap uncertainty set into an additive structure is indicated in the following two propositions. First it will be shown that the set of frequency responses of plants $G_\Delta \in G_\nu(G_x, W_\nu)$ (see (3)) can equivalenty be described in terms of a linear fractional transformation.

Proposition 2 *Define the set $\overline{G}_\nu(G_x, W_\nu)$ as*

$$\left.\begin{aligned}\overline{G}_\nu(G_x,W_\nu) := \{G_\Delta \mid \\ G_\Delta = \frac{\bar{N}_x(s) + \bar{D}_{G_x^*}(s)\Delta_G(s)}{\bar{D}_x(s) - \bar{N}_{G_x^*}(s)\Delta_G(s)}, \\ \text{with } |\Delta_G(i\omega)| \le \frac{|W_\nu(i\omega)|}{\sqrt{\left(1-|W_\nu(i\omega)|^2\right)}} \quad \forall \omega \in \mathbb{R}\end{aligned}\right\}$$

with $(\bar{N}_x, \bar{D}_x)$ and $\left(\bar{N}_{G_x^*}, \bar{D}_{G_x^*}\right)$ normalized coprime factorizations of G_x and G_x^*, respectively.
Then it holds that $G_\nu(G_x, W_\nu) = \overline{G}_\nu(G_x, W_\nu)$.

Proof Every plant G_Δ can be represented as $G_\Delta = \left(\bar{N}_x + \bar{D}_{G_x^*}\Delta_G\right)\left(\bar{D}_x - \bar{N}_{G_x^*}\Delta_G\right)^{-1}$ by a unique Δ_G given by

$$\begin{aligned}\Delta_G &= -\left(\bar{D}_\Delta \bar{D}_{G_x^*} + \bar{N}_\Delta \bar{N}_{G_x^*}\right)^{-1}\left(\bar{D}_\Delta \bar{N}_x - \bar{N}_\Delta \bar{D}_x\right) \\ &= \bar{D}_{G_x^*}^{-1}\left(1 + G_\Delta G_x^*\right)^{-1}\left(G_\Delta - G_x\right)\bar{D}_x.\end{aligned}$$

From the definition in equation (3) it holds that

$$\begin{aligned}\kappa(G_\Delta, G_x) &= \left|\begin{bmatrix} -\bar{D}_x & \bar{N}_x \end{bmatrix}\begin{bmatrix} \bar{N}_x + \bar{D}_{G_x^*}\Delta_G \\ \bar{D}_x - \bar{N}_{G_x^*}\Delta_G \end{bmatrix} Q^{-1}\right| \\ &= \left|\bar{D}_x \bar{D}_{G_x^*} + \bar{N}_x \bar{N}_{G_x^*}\right| |\Delta_G| \left|Q^{-1}\right|, \end{aligned} \tag{8}$$

with Q the normalizing factor given as the spectral factor of

$$\begin{aligned}Q^*Q = &\left(\bar{N}_x + \bar{D}_{G_x^*}\Delta_G\right)^*\left(\bar{N}_x + \bar{D}_{G_x^*}\Delta_G\right) \\ &+ \left(\bar{D}_x - \bar{N}_{G_x^*}\Delta_G\right)^*\left(\bar{D}_x - \bar{N}_{G_x^*}\Delta_G\right).\end{aligned}$$

Using the facts that

$$\begin{aligned}&\bar{N}_x^*\bar{N}_x + \bar{D}_x^*\bar{D}_x = 1\ ,\ \ \bar{D}_{G_x^*}^*\bar{D}_{G_x^*} + \bar{N}_{G_x^*}^*\bar{N}_{G_x^*} = 1 \\ &\bar{D}_{G_x^*}^*\bar{N}_x - \bar{N}_{G_x^**}^*\bar{D}_x = \bar{D}_{G_x^*}^*\left(G_x - (G_x^*)^*\right)\bar{D}_x = 0\end{aligned} \tag{9}$$

the expression for Q^*Q reduces to $Q^*Q = 1 + \Delta_G^*\Delta_G$.
Further, by division of (9) by the product of denominator factors, it follows that

$$\bar{D}_x^*\bar{D}_x = \left(G_x^*G_x + 1\right)^{-1}, \qquad \bar{D}_{G_x^*}^*\bar{D}_{G_x^*} = \left(G_xG_x^* + 1\right)^{-1},$$

showing that

$$\begin{aligned}\left|\bar{D}_x\bar{D}_{G_x^*} + \bar{N}_x\bar{N}_{G_x^*}\right|^2 &= \left|1 + G_xG_x^*\right|^2\left|\bar{D}_x\bar{D}_{G_x^*}\right|^2 \\ &= \left|1 + G_xG_x^*\right|^2\left|1 + G_xG_x^*\right|^{-2} = 1.\end{aligned}$$

Expression (8) then becomes

$$\kappa(G_\Delta, G_x) = \frac{|\Delta_G|}{\sqrt{1+|\Delta_G|^2}}, \tag{10}$$

from which it follows that $|\Delta_G| = \dfrac{\kappa(G_\Delta, G_x)}{\sqrt{1-\kappa^2(G_\Delta, G_x)}}$. □

The LFT representation of the ν-gap set $G_\nu(G_x, W_\nu)$ of Proposition 2 immediately reveals the circular properties of $G_\nu(G_x, W_\nu)$ in the frequency domain, which is formalized in the following proposition.

Proposition 3 *The set of frequency responses of all plants $G_\Delta \in G_\nu(G_x, W_\nu)$ (as defined in (3)) is equivalently described as an additive uncertainty set $G_a(G_{centre}, W_a)$ (see (1)) with*

$$G_{centre} = \frac{G_x}{1-\left(1+|G_x|^2\right)|W_\nu|^2}$$
$$W_a = \frac{\sqrt{\left(1-|W_\nu|^2\right)}\left(|G_x|^2+1\right)W_\nu}{1-\left(1+|G_x|^2\right)|W_\nu|^2}.$$

Proof See appendix. □

The fact that both the Youla uncertainty set and the ν-gap uncertainty set allow for an additive description shows that the two sets can be transformed into one another. That both uncertainty structures induce circular uncertainty regions in the frequency domain could be gathered from existing literature, see e.g. [34] for the ν-gap structure. However, the explicit formulations of the uncertainty sets in terms of an additive structure allows for a thorough comparison, as is further explored in the subsequent section.

4.2 *Transfer functions in the uncertainty sets*

The preceding section showed how a union of circles in the frequency domain describing a set of frequency responses is independent of a particular uncertainty structure, when allowing for different nominal models and weighting functions. This result is very useful when evaluating robust performance analysis and synthesis since the control performance specification of expression (4) can be evaluated solely on the basis of frequency responses (cf. Section 6). However, a robust stability evaluation (cf. Section 5) is in terms of transfer functions. To formulate robust stability conditions additional constraints have to be imposed in terms of unstable poles and zeros. Each of the three structures is accompanied by a condition on unstable poles/zeros induced by the standard robust stability criteria (cf. Section 5). In particular,

- additive structure: $\Delta_a(s) \in \mathbb{R}H_\infty$ or $\eta(G_\Delta(s)) = \eta(G_x(s))$ (with $\eta(\cdot)$ denoting the number of unstable poles) [35].
- Youla structure: $\Delta_G(s) \in \mathbb{R}H_\infty$ [33].
- ν-gap structure: $wno(\bar{N_x}^*(s)\bar{N_\Delta}(s) + \bar{D_x}^*(s)\bar{D_\Delta}(s)) = 0$. (with $wno(g)$ denoting the winding number about the origin of $g(s)$ as s follows the standard Nyquist D-contour) [34].

With each of these particular conditions on the transfer functions a different subset is obtained from all possible frequency responses in the union of circles. However, it can be shown that even under the above constraints each point in the union of circles can be reached with all three uncertainty structures. In particular, the associated subset of frequency responses is such that, at each frequency ω, every point within and on the boundary circle is reached for at least one plant $G_\Delta(s)$ in the set (see Figure 4). This is formalized in the following propositions.

Proposition 4 *Consider the additive set $G_a(G_x, W_a)$ as defined in (1) subject to the additional constraint $\eta(G_\Delta) = \eta(G_x)$. Then for every $\omega \in \mathbb{R}$ and $r \leq |W_a(i\omega)|$ and $0 \leq \phi < 2\pi$ there exists a $G_\Delta(s)$ in the constrained set such that $G_\Delta(i\omega) - G_x(i\omega) = re^{i\phi}$.*

Proof A suitable transfer function $G_\Delta(s)$ can always be found and could be formed as $G_\Delta = G_x(s) + \Delta_a(s)$ with $\Delta_a(s)$ a stable inner function giving a particular amplitude and phase shift at, say, ω_k. In particular, the stable inner function

$$\Delta_{\zeta,\beta}(s) = \beta\left(\frac{s-\zeta}{s+\zeta}\right)^4, \tag{11}$$

with

$$\zeta = \frac{-\omega_k}{\tan\frac{\phi}{4}}\left(1 \pm \sqrt{\left(1+\tan^2\frac{\phi}{4}\right)}\right), \tag{12}$$

has an amplitude of β over all frequency and a ω-dependent phase ϕ. The fourth order allows for a phase shift over the

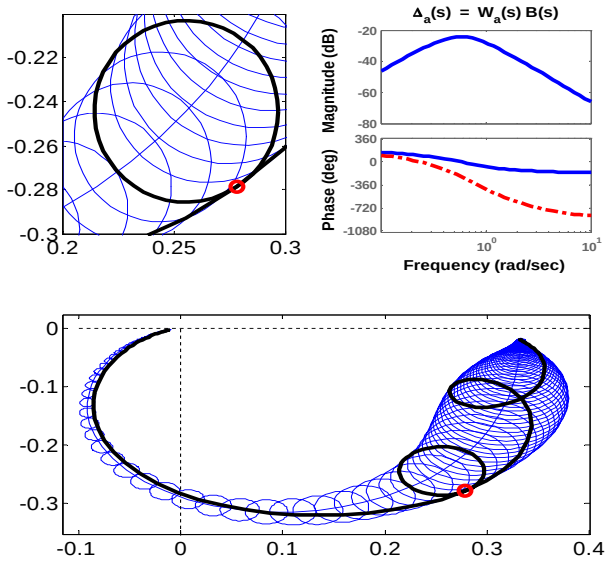

Fig. 4. Consider a union of circles in the frequency domain associated with the additive set $G_a(G_x, W_a)$. At each frequency ω, every point within and on the boundary circle (top left) is reached for at least one $G_\Delta(s) \in G_a(G_x, W_a)$ satisfying $\eta(G_\Delta) = \eta(G_x)$. For example, $G_\Delta(s) = G_x(s) + \Delta_a(s)$, depicted as the thick curve in the bottom plot, with $\Delta_a = W_a(s)B(s)$ and $B(s)$ a suitable inner function. The top right plot shows the Bode plots of W_a (solid blue) and Δ_a (dashed red).

complete 2π radians. If β is chosen between 0 and 1 the stable transfer function $W_a\Delta_a(\zeta)$ will have an amplitude equal to or smaller than $|W_a(i\omega)|$, $\forall\omega \in \mathbb{R}$, and at a particular frequency ω_k any phase can be obtained.

In particular, the frequency response of $\Delta_{\zeta,\beta}(s) = \beta\left(\frac{s-\zeta}{s+\zeta}\right)$ has a phase ϕ at ω_k when ζ is chosen as

$$\zeta = \frac{-\omega_k}{\tan\phi}\left(1 \pm \sqrt{(1+\tan^2\phi)}\right), \tag{13}$$

which follows from the fact that

$$\mathrm{Re}\left(\Delta_{\zeta,\beta}(i\omega_k)\right) = \beta\frac{\omega_k^2-\zeta^2}{\omega_k^2+\zeta^2}; \quad \mathrm{Im}\left(\Delta_{\zeta,\beta}(i\omega_k)\right) = \beta\frac{2\omega_k\zeta}{\omega_k^2+\zeta^2}$$

and

$$\tan\phi = \frac{2\omega_k\zeta}{\omega_k^2-\zeta^2},$$

which is solved for ζ in expression (13). Result (12) for the fourth order inner function of (11) follows easily. Technically, the required $\Delta_{\zeta,\beta}$ could violate the condition $\eta(G_\Delta) = \eta(G_x)$ by cancelling an unstable pole in G_x, in which case an additional inner function could be used changing the required phase and associated $\Delta_a(\zeta)$. □

Proposition 5

a) Consider the set of plants $G_Y(G_x,C,Q,Q_c,W_Y)$ as defined in (2) subject to the additional constraint $\Delta_G(s) \in \mathbb{R}H_\infty$. Then for every $\omega \in \mathbb{R}$ and $r \leq |W_a(i\omega)|$ and $0 \leq \phi < 2\pi$ there exists a $G_\Delta(s)$ in the constrained set such that $G_\Delta(i\omega) - G_x(i\omega) = re^{i\phi}$, with G_x and W_a as defined in Corollary 1.

b) Consider the set of plants $G_\nu(G_x,W_\nu)$ as defined in (3) subject to the additional constraint $wno(N_x^*(s)N_\Delta(s) + D_x^*(s)D_\Delta(s)) = 0$. Then for every $\omega \in \mathbb{R}$ and $r \leq |W_a(i\omega)|$ and $0 \leq \phi < 2\pi$ there exists a $G_\Delta(s)$ in the constrained set such that $G_\Delta(i\omega) - G_x(i\omega) = re^{i\phi}$, with G_x and W_a as defined in Corollary 3.

Proof Proposition 2 showed that the set of frequency responses $\bar{G}_\nu(G_x,W_\nu)$ equals those of the ν-gap set $G_\nu(G_x,W_\nu)$. Further, all transfer functions $G_\Delta(s) \in \bar{G}_\nu(G_x,W_\nu)$ satisfying $\Delta_G \in \mathbb{R}H_\infty$ satisfy the winding number condition $wno(N_x^*(s)N_\Delta(s) + D_x^*(s)D_\Delta(s)) = 0$, since

$$\begin{aligned} wno(\bar{N}_x^*\bar{N}_\Delta + \bar{D}_x^*\bar{D}_\Delta) = \\ wno(1 + \left(\bar{N}_x^*\bar{D}_{G_x^*} - \bar{D}_x^*\bar{N}_{G_x^*}\right)\Delta_G) + wno(Q^{-1}) = \\ wno(1 + \bar{D}_x^*\left(\bar{G}_x^* - \bar{G}_x^*\right)\bar{D}_{G_x^*}\Delta_G) + wno(Q^{-1}) = \\ wno(1) + wno(Q^{-1}) = 0. \end{aligned}$$

In other words, the set of plants $G_\Delta(s) \in \bar{G}_\nu(G_x,W_\nu)$ satisfying $G_\Delta \in \mathbb{R}H_\infty$ forms a subset of the set of transfer functions $G_\Delta \in \bar{G}_\nu(G_x,W_\nu)$ satisfying the winding number condition. Now, since the mappings of $G_\Delta(s) = \frac{\bar{N}_x(s)+\bar{D}_c(s)\Delta_G(s)}{\bar{D}_x(s)-\bar{N}_c(s)\Delta_G(s)}$ and $G_\Delta = \frac{\bar{N}_x(s)+\bar{D}_{G_x^*}(s)\Delta_G(s)}{\bar{D}_x(s)-\bar{N}_{G_x^*}(s)\Delta_G(s)}$ are bijective, implying that for every (stable) Δ_G there is a unique G_Δ and vice versa, the proof of Proposition 4 can be followed for dual Youla and ν-gap as well. While in the proof for the additive case care has to be taken that the term Δ_a does not induce a cancellation of unstable poles of G_x, for the ν-gap the term Δ_G should not violate coprimeness (in dual Youla this is automatically taken care of by requiring Δ_G to be stable). □

The above propositions show that pole/zero conditions imposed on the transfer functions in the uncertainty sets do not induce any restrictions in terms of the points that can be reached in the circular region at each frequency. Within the 'tube' induced by the union of circles over frequency not every frequency response can be allowed because of the pole/zero condition. However, the boundary of the circles is always reached by at least one plant of the set. This fact is very relevant for robustness studies of the constrained sets of plants. It implies that robustness tests in the frequency domain can be applied without conservatism to the union of circles in the complex plane, irrespective of the particular constraints on unstable poles/zeros.

4.3 Identification of model uncertainty sets

The preceding section showed how a circular region in the frequency domain is equivalently described in terms of an additive, dual Youla and ν-gap uncertainty structure. In an identification setting we think of the uncertainty regions as resulting from an identification experiment. These can e.g. be ellipsoidal or boxed regions following from the methods of [9,18,17,25,16]. In order to provide uncertainty sets that are suited to be used as a basis for control design and evaluation, appropriately structured uncertainty sets are required such as the structures discussed before (additive, Youla, ν-gap). Consequently they need to embed the uncertainty regions that result from identification. In identification for control, the choice of uncertainty structure seems to be an important user's choice [32]. However, the equivalence of the several structures as presented here, implies that the smallest (unique) circle embedding the identification uncertainty can equivalently be described in all structures of Section 2. As a result there are no arguments favouring one structure over another. Each representation, however, will have a different nominal model and weighting function.

In identification for control it is common practice to first identify a (low order) nominal model, and subsequently to bound the uncertainty around this nominal model [13,31,1]. When fixing the nominal model, embedding the identified uncertainty set will result in different regions for the different uncertainty structures. In other words: in order to maintain the advantages of the equivalence of structures, both nominal model and weighting functions have to be made flexible. As a result, the principal problem in identification for control appears to be an uncertainty set estimation, minimizing over both nominal model and uncertainty bound, rather than first identifying a nominal model (with any method) and subsequently bounding the model uncertainty. This builds on earlier results as discussed in [32,6].

In general, however, embedding is sought while maintaining a particular nominal model, in which case all structures will provide different embedding regions. Propositions 1, 3 and Corollary 1 show how the circular uncertainty region increases in size with increasing W_a, W_Y, W_ν, respectively. But moreover, they show that for a fixed nominal model G_x the uncertainty regions expand with increasing W in a particular way, i.e. the centre of the circular sets moves along a particular line while the circles expand. Figure 5 illustrates how an additive uncertainty set $\bar{G}_a(G_x,W_a)$ increases with W_a in concentric circles around G_x. The centre of the dual Youla uncertainty set $\bar{G}_Y(G_x,C,Q,Q_c,W_Y)$ moves along the line between G_x and $-C^{-1}$ away from $-C^{-1}$ as the uncertainty level W_Y increases. Note from Corollary 1 that at $|\bar{W}_Y|^2 = 1$, the centre passes through infinity after which it continues to move alone the line through G_x and $-C^{-1}$ towards $-C^{-1}$. In this case, the set is given by the exterior of the boundary circle whose radius is now seen to decrease with increasing uncertainty W_Y. Similarly, the centre of the ν-gap set $\bar{G}_\nu(G_x,W_\nu)$ moves along the line between G_x and $-(G_x^*)^{-1}$ away from $-(G_x^*)^{-1}$ (cf. Proposition 2).

Note the significance of the points $-C^{-1}$ and $-(G_x^*)^{-1}$, respectively, for the dual Youla and ν-gap uncertainty. When, for fixed G_x, plant models need to be described that are close

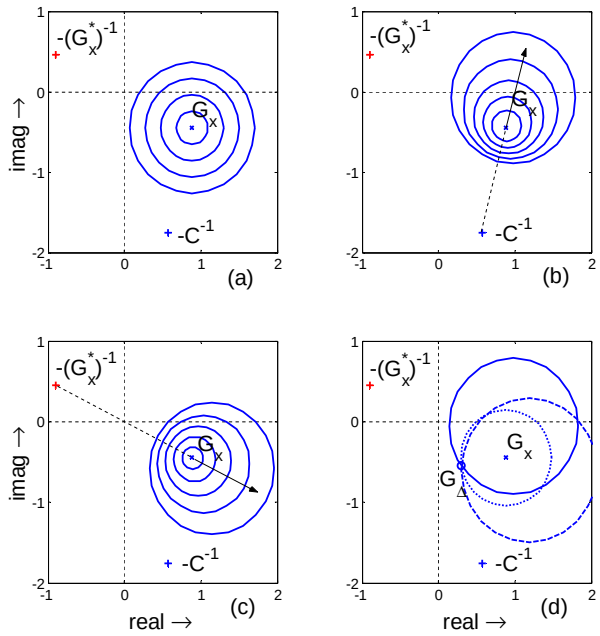

Fig. 5. Illustration of the characteristics of an additive, dual Youla and ν-gap uncertainty structure with respect to a fixed nominal model G_x. Figures a,b and c depict contours of increasing additive, dual Youla and ν-gap uncertainty around G_x, respectively. While the contours are concentric for the additive uncertainty, for the dual Youla uncertainty the centre of the set shifts with increasing uncertainty along a line between G_x and $-C^{-1}$ away from $-C^{-1}$. Similarly, the ν-gap set is seen to increase with a centre shifting along a line between G_x and $-(G_x^*)^{-1}$ away from $-(G_x^*)^{-1}$. Figure d illustrates the differences when embedding a plant G_Δ with the smallest additive set (dotted), the smallest ν-gap set (dashed) and the smallest dual Youla set (solid) around the nominal model G_x.

to these points, the radii of the uncertainty sets will need to be large. In other words, the uncertainty structures are most sensitive in the direction of these respective points. For additive uncertainty, this same reasoning holds with respect to the point $(0)^{-1}$. For example, in Figure 6 it is indicated how an additive set $G_a(G_x,W_a)$ with nominal model G_x, can be embedded by a ν-gap set $G_\nu(G_x,W_\nu)$ with the same nominal model G_x. When building a ν-gap set around nominal model G_x, the centre of the resulting circular region moves along the line through G_x and $-(G_x^*)^{-1}$. This can be understood by examining the expression for G_{centre} in Proposition 3 or Proposition 2. Consequently, in order to cover $G_a(G_x,W_a)$, W_ν has to be increased until the circular ν-gap region touches the additive set $G_a(G_x,W_a)$ in that point on the boundary of the circle that intersects the line from $-(G_x^*)^{-1}$ to G_x. In other words, the point closest to $-(G_x^*)^{-1}$ corresponds to that element from $G_a(G_x,W_a)$ which accounts for the largest chordal distance from G_x. Additionally, Proposition 3 shows that a ν-gap set $G_\nu(G_x,W_\nu)$ cannot embed an additive set $G_a(G_x,W_a)$ which contains the point $-(G_x^*)^{-1}$, since the

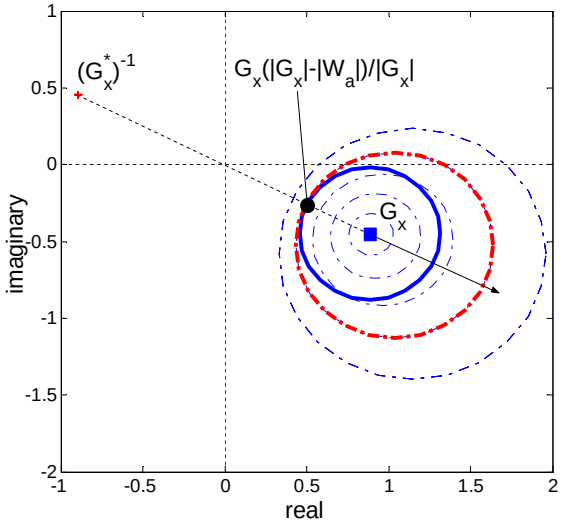

Fig. 6. Embedding an additive uncertainty $G_a(G_x,W_a)$ (blue solid) with a ν-gap uncertainty (red dashed-dot). Contour lines corresponding to ν-gap sets $G_\nu(G_x,W_\nu)$ with increasing W_ν are depicted by the thin dashed-dotted lines similar to those in Figure 5.c. The point $G_x(|G_x|-|W_a|)/|G_x|$ in line with the nominal model G_x ('□') will cause the largest chordal distance from G_x among all elements of $G_a(G_x,W_a)$.

point $-(G_x^*)^{-1}$ is only reached for $W_\nu = 1$. These results provide an analytical tool to calculate the chordal distance over an additive uncertainty set with a nominal model G_x. Similarly as above, a quantitative comparison can be made between any of the three uncertainty structures using the results of Proposition 1 and 3 and Corollary 1.

5 Robust stability

5.1 *Robust stability and the frequency domain*

Constraints on unstable poles and zeros as in Section 4.2 are required for the formulation of conditions for robust stability, i.e. the question whether a controller $C(s)$ stabilizes all elements $G_\Delta(s) \in G$. For example, a controller $C(s)$, satisfying the condition $\left|C(i\omega)(1+C(i\omega)G_x(i\omega))^{-1}\right| < \left|W_a^{-1}(i\omega)\right|$, stabilizes the additive set $G_a(G_x,W_a)$ provided that $G_x(s)$ is stabilized by $C(s)$ and all elements of $G_a(G_x,W_a)$ have an equal number of unstable poles. In such results for robust stability three types of conditions can be discerned:

i. the condition that $C(i\omega) \neq -G_\Delta^{-1}(i\omega)$ for all $G_\Delta(i\omega) \in G$ and for all $\omega \in \mathbb{R}$.
ii. the condition that C stabilizes a nominal model $G_x \in G$.
iii. conditions on all $G_\Delta \in G$ with respect to the nominal model G_x.

The first condition on the frequency responses seems most characteristic for different uncertainty structures:

a) $\left|C(i\omega)(1+C(i\omega)G_x(i\omega))^{-1}\right| < \left|W_a^{-1}(i\omega)\right|$ for the additive uncertainty structure [35],
b) $\left|Q^{-1}(i\omega)\Delta_G(i\omega)Q_c(i\omega)\right| \leq \left|W_Y^{-1}(i\omega)\right|$ for the dual Youla uncertainty structure [29,12] and
c) $\overline{\sigma}(T(C(i\omega),G_x(\omega)) < \left|W_\nu^{-1}(i\omega)\right|$ for the ν-gap uncertainty [34].

However, they are simply ensuring the condition that $C(i\omega) \neq -G_\Delta^{-1}(i\omega)$ for all $G_\Delta(i\omega) \in G$. And from the preceding sections it is clear that all three uncertainty sets can be transformed into one another with respect to the frequency responses of the members. Naturally the 'nominal' model and weighting function will change. For example, part *i*. of the robust stability condition for the ν-gap set $\overline{\sigma}(T(C(i\omega),G_x(i\omega)) < \left|W_\nu^{-1}(i\omega)\right|$, is equivalently described by the (additive) condition $\left|C(1+CG_{centre})^{-1}\right| < \left|W_a^{-1}\right|$, with G_{centre} and W_a as formulated in Proposition 3. The uncertainty sets do differ in terms of part *iii*. That is, they differ in terms of a winding number condition or a condition on unstable poles and zeros.

5.2 Identification and robust stability

Many identification techniques characterize the plant identification uncertainty in terms of bounds on the frequency response, see e.g. [9,16,18,2,28]. The discussion in Section 4.3 showed that such a set of frequency responses is equivalently described in any of the uncertainty structures. When considering robust stability, however, the uncertainty sets do differ in terms of winding-number/pole/zero condition, i.e. each uncertainty structure induces a different subset of transfer functions associated with the identified set of frequency responses. The question arises whether system identification provides for information to determine which of the winding-number/pole/zero constraints are satisfied and correspondingly which of the uncertainty structures has to be chosen to describe the plant uncertainty. Identification methods generally do not operate under particular winding-number/pole/zero constraints on the resulting models. With one major exception: the constraint that the identified object is stable. The constraint of stable models is regularly applied in identification either in an open-loop setting or in closed-loop identification. In other words, the verification of condition *iii*. is feasible for an additive uncertainty structure following an open-loop identification which requires that all elements $G_\Delta \in G_a(G_x,W_a)$ are stable. Or, a closed-loop identification could lead to a Youla parameter uncertainty where a stability condition on Δ_G can automatically be satisfied, since the Youla parameter itself can directly be identified from closed-loop data [30].

6 Robust performance analyis

A controller is said to perform robustly for a set of plants if a certain performance level is reached for all plants in the uncertainty set. A robust performance analysis comes down to a worst-case performance evaluation over the uncertainty set. To this end, nonlinear optimization or LMI based procedures are available for general (LFT based) uncertainty structures [35]. For SISO systems with a one dimensional uncertainty block, bounded in amplitude, these tools provide for a nonconservative answer. However, in the following we will derive analytical expressions since this will allow for more insight. In case non-circular uncertainty regions are considered, in some cases an adapted μ-analysis could be employed, as for ellipsoidal regions [2], but in general standard techniques are not applicable. Here we will not consider non-circular regions.

6.1 One-block performance functions

First scalar performance specifications are considered. That is, the weighting functions V and W of the performance measure (4) are such that only one element of the function matrix $T(G_\Delta,C)$ of expression (5) is selected. The performance of a (circular) uncertainty set with a particular controller will be analyzed using the results of Section 3. The discussion is facilitated by considering a particular example. Consider a plant G_x controlled by a controller C, and in the performance cost consider $V = W = diag(0,1)$, such that

$$J(G_x,C) = \left|\frac{1}{1+G_x(i\omega)C(i\omega)}\right|.$$

We will study the effect of an, say additive, uncertainty in G_x on the performance with C. First of all, Proposition 1 provides for an exact description of the performance of all elements of the uncertainty set. The set of all sensitivity functions induced by the controller C and the additive uncertainty set $G_a(G_x,W_a)$ is given by

$$S_\Delta = \frac{1}{1+(G_x+\Delta_a)C}, \quad \left|W_a^{-1}\Delta_a\right| \leq 1, \quad \text{or} \tag{14}$$
$$= (1+G_xC)^{-1} - \frac{(1+G_xC)^{-2}C\Delta_a}{1+(1+G_xC)^{-1}C\Delta_a}, \quad \left|W_a^{-1}\Delta_a\right| \leq 1.$$

Proposition 1 provides for the following alternative description of this set,

$$S_\Delta = S_{centre} + \Delta_S, \quad |\Delta_S| \leq |W_S| \text{ with} \tag{15}$$
$$S_{centre} = \frac{(1+CG_x)^{-1}}{1-\left|(1+CG_x)^{-1}CW_a\right|^2} \text{ and}$$
$$W_S = \frac{(1+CG_x)^{-2}C}{1-\left|(1+CG_x)^{-1}CW_a\right|^2}W_a,$$

which follows from the fact that the set (15) equals the LFT $F(P,\Delta)$ of Proposition 1 with the entry P containing both the controller C and the nominal plant G_x, i.e. $P_{22} = (1+G_xC)^{-1}$, $P_{12}P_{21} = (1+G_xC)^{-2}C$ and $P_{11} = (1+G_xC)^{-1}C$.

The circular representation (15) allows for a straightforward robust performance analysis. The minimal and maximal (worst-case) performance cost at each frequency can be expressed analytically by

$$\max_{\Delta_a,\left|W_a^{-1}\Delta_a\right|\leq 1} |S_\Delta| = |S_{centre}| + |W_S| \tag{16}$$

$$\min_{\Delta_a,\left|W_a^{-1}\Delta_a\right|\leq 1} |S_\Delta| = |S_{centre}| - |W_S|\,. \tag{17}$$

From the discussion after Proposition 1 it can be concluded that an increase of the uncertainty (W_a) at a particular frequency will always lead to an increase of the worst-case performance cost at that same frequency. Expression (15) provides for the exact amount of performance degradation (increase of worst-case performance) with growing uncertainty.
The example also shows that part i. of the robust stability condition given in Section 5 appears naturally in the denominators of the centre and the weighting function. That is, to maintain a finite performance cost for all elements in the additive uncertainty set considered here, the associated (small gain) condition $\left|(1+CG_x)^{-1}CW_a\right| < 1$ has to be satisfied.
Finally, note that the nominal sensitivity $S_x = (1+CG_x)^{-1}$ is not the centre of the set of sensitivity functions S_Δ. This property becomes critically important when considering non-circular boundaries and/or probability density functions over the uncertainty set (see the discussion in Section 3.2).
All of the above observations hold true for any of the three uncertainty structures (additive, Youla and ν-gap) and a one-block performance measure (4) with a particular controller C. Most importantly, the worst-case performance cost at each frequency can be calculated analytically.

The Youla parameter uncertainty structure plays a special role in case we consider the robust performance of the auxiliary controller C used in the parametrization itself (i.e. the "present" controller). For this auxiliary controller all four scalar entries of $T(G_\Delta,C)$ over the set $G_Y(G_x,C,Q,Q_c,W_Y)$ are affine in the uncertainty Δ_G. With the coprime factors of G_Δ, G_x and C as in the dual Youla expression (2), the performance matrix $T(G_\Delta,C)$ of expression (5) becomes ([31])

$$\begin{aligned}
T(G_\Delta,C) &= \begin{bmatrix} N_\Delta \\ D_\Delta \end{bmatrix} (\bar{D}_c D_\Delta + \bar{N}_c N_\Delta)^{-1} \begin{bmatrix} \bar{N}_c & \bar{D}_c \end{bmatrix} \\
&= \begin{bmatrix} \bar{N}_x + \bar{D}_c\Delta_G \\ \bar{D}_x - \bar{N}_c\Delta_G \end{bmatrix} \cdot \\
&\quad (\bar{D}_c\bar{D}_x - \bar{D}_c\bar{N}_c\Delta_G + \bar{N}_c\bar{N}_x + \bar{N}_c\bar{D}_c\Delta_G)^{-1} \begin{bmatrix} \bar{N}_c & \bar{D}_c \end{bmatrix} \\
&= T(G_x,C) + \begin{bmatrix} \bar{D}_c \\ \bar{N}_c \end{bmatrix} \Delta_G (\bar{D}_c\bar{D}_x + \bar{N}_c\bar{N}_x)^{-1} \begin{bmatrix} \bar{N}_c & \bar{D}_c \end{bmatrix}.
\end{aligned}$$

This implies that the nominal performance will be the centre of the set of performance functions associated with $G_Y(G_x,C,Q,Q_c,W_Y)$. Moreover, probability density functions and non-circular uncertainty structures (e.g. boxed/ellipsoidal/irregular) maintain their shape under the mapping from G_Y to the performance cost functions.

6.2 Multi-block performance function

For non-scalar performance functions, i.e. for general diagonal weighting functions V and W in the performance measure (4), Proposition 1 cannot be used. Still, an analytical expression can be formulated for the worst-case performance of a controller over a circular uncertainty set. To this end, first the following Lemma is presented in which the performance cost $J(G_\Delta,C,V,W)$ is expressed in terms of the sensitivity function of the closed loop of G_Δ and C. A similar result but without the inclusion of weighting matrices is derived in [34] in connection with loop-shaping.

Lemma 1 *For the performance measure $J(G_\Delta,C,V,W)$ of expression (4) it holds that at each frequency* ω

$$\begin{aligned}
&J(G_\Delta,C,V,W)^2 = \bar{\sigma}(VT(G_\Delta,C)W)^2 = \\
&\left(\left(S_\Delta - \frac{|V_1|^2}{\left(|V_1|^2+|V_2|^2|C|^2\right)}\right)\left(S_\Delta - \frac{|V_1|^2}{\left(|V_1|^2+|V_2|^2|C|^2\right)}\right)^* + \right. \\
&\left.\frac{|V_1|^2|V_2|^2|C|^2}{\left(|V_1|^2+|V_2|^2|C|^2\right)^2}\right) \frac{\left(|V_1|^2+|V_2|^2|C|^2\right)\left(|W_2|^2+|W_1|^2|C|^2\right)}{|C|^2},
\end{aligned} \tag{18}$$

where $S_\Delta = (1+CG_\Delta)^{-1}$, $V = diag(V_1,V_2)$ and $W = diag(W_1,W_2)$.

Proof See appendix. □

Analyzing expression (18) it is seen that the performance measure $J(G_\Delta,C,V,W)^2$ can be interpreted as the 'height' of a three-dimensional parabola over the (complex) variable S_Δ. Figure 7 depicts the parabola centred at $\frac{|V_1|^2}{\left(|V_1|^2+|V_2|^2|C|^2\right)}$. Note that the value of $J(G_\Delta,C,V,W)^2$ increases whenever S_Δ is moving away from the centre $\frac{|V_1|^2}{\left(|V_1|^2+|V_2|^2|C|^2\right)}$ and that all S_Δ at an equal distance from the centre induce the same value $J(G_\Delta,C,V,W)^2$. In other words, given a set of sensitivity functions S_Δ for a particular controller C, the sensitivity function S_{WC} associated with the largest (worst-case) performance cost is easily identified as the one most removed from the centre $\frac{|V_1|^2}{\left(|V_1|^2+|V_2|^2|C|^2\right)}$.

A result similar to Lemma 1 can also be derived in terms of the complementary sensitivity or any of the other terms in $T(G_\Delta,C)$. However, the specific formulation in terms of the sensitivity function is chosen because expression (18) is such that the plant G_Δ enters in none of the terms other than the term S_Δ, which facilitates the explicit expression of the performance cost; for example the centre of the parabola is G_Δ-independent which property is lost in the other cases. The

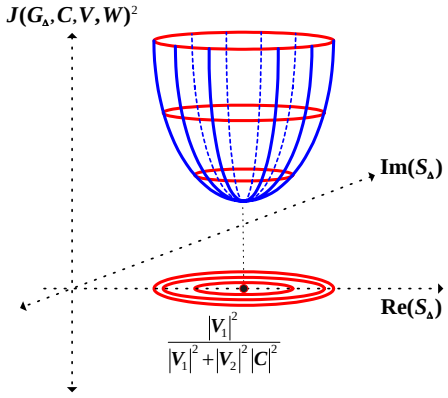

Fig. 7. The performance cost $J(G_\Delta,C,V,W)^2$ at a given frequency ω can be interpreted as the 'height' of a three-dimensional parabola over the (complex) variable S_Δ. The projection of the level sets of the parabola onto the plane of $\mathrm{Re}(S_\Delta)$ and $\mathrm{Im}(S_\Delta)$ is circular and centred around $|V_1|^2\left(|V_1|^2+|V_2|^2|C|^2\right)^{-1}$.

worst-case performance can now be calculated following a two-step approach:

- In the first step the set of plants G is mapped with the controller C into a set of sensitivity functions $S(G,C)$.
- The second step is provided by Lemma 1 which shows that the worst-case performance is achieved for that particular $S_{WC} \in S(G,C)$ most removed from the 'centre' $|V_1|^2/\left(|V_1|^2+|V_2|^2|C|^2\right)$.

For a (circular) uncertainty set G the set $S(G,C)$ can be given an additive structure by application of Proposition 1, i.e $S(G,C) := \{S_\Delta \mid S_\Delta = S_{centre}+\Delta_S\ ,\ |W_S^{-1}\Delta_S| < 1\}$ (cf. expression (15)), allowing for an analytical computation of S_{WC} and the associated worst-case performance value. This is illustrated in Figure 8 and formalized in the following corollary.

Corollary 2 *Let there be a set of plants G in either the additive, dual Youla or ν-gap uncertainty structure and consider the performance cost $J(G_\Delta,C,V,W)$ of (4). For a given controller C the set of plants G is mapped into a set of sensitivity functions $S(G,C)$, which can be described in an additive structure using Proposition 1 as*

$$S(G,C) := \left\{S_\Delta \ \mid\ S_\Delta = S_{centre}+\Delta_S\ ,\ |W_S^{-1}\Delta_S| \le 1\right\}.$$

At each frequency the particular $S_{WC} \in S(G,C)$ that yields the worst-case performance cost of $J(G_\Delta,C,V,W)$ over all $G_\Delta \in G$, is given by

$$S_{WC} = S_{centre} + |W_S| \exp\left(i\tan^{-1}\left(\frac{Im\,(S_{centre})}{Re\,(S_{centre}) - \frac{|V_1|^2}{\left(|V_1|^2+|V_2|^2|C|^2\right)}}\right)\right).$$

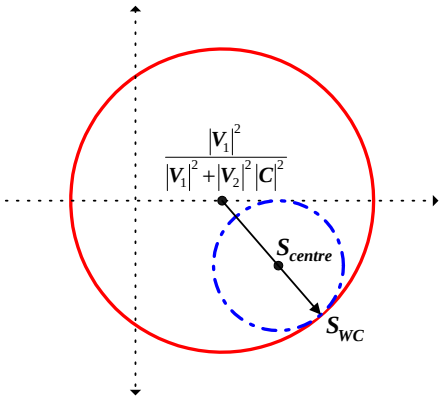

Fig. 8. 2-D projection of the performance cost $J(G_\Delta,C,V,W)$ depicted in Figure 7 illustrating the worst-case performance calculation. An uncertainty set G induces with a controller C a set of sensitivity functions $S(G,C)$ (blue dashed-dotted circle). Lemma 1 shows that the worst-case performance is achieved for that particular $S_{WC} \in S(G,C)$ most removed from the 'centre' $\frac{|V_1|^2}{|V_1|^2+|V_2|^2|C|^2}$.

The exact value of the worst-case performance cost follows from inserting S_{WC} in expression (18) of Lemma 1.

Proof The corollary follows from the circular nature of the three uncertainty structures (Corollary 1 and Proposition 3), the fact that the boundary of circular region at each frequency is reached for at least one member of the uncertainty set (Propositions 4 and 5), from the application of Proposition 6 and Lemma 1 and standard geometric considerations. □

6.3 *Comparing uncertainty sets in terms of performance cost*

The previous section provided for an analytical approach of calculating the worst-case performance of a controller C over a plant uncertainty set by mapping the set of plants to a set of sensitivity functions. In this section an opposite approach is taken in order to study the differences between the three uncertainty sets of Section 2. Starting from a given performance cost $J(G_\Delta,C,V,W)$ all plants are characterized achieving this cost with a given controller C. The three uncertainty sets are then compared with this set of all plants achieving the particular performance cost.
Lemma 1 can be read as to give a description of all sensitivity functions achieving $\bar{\sigma}(VT(G_\Delta,C)W) < \gamma$. Figure 7 illustrates that the projection of a horizontal intersection of the parabola, depicted by the solid circle in Figure 8, is the set of all sensitivity functions achieving the performance corresponding to the level of the intersection. This is formalized in the following corollary,

Corollary 3 *The set of all sensitivity functions $S_\Delta = (1+CG_\Delta)^{-1}$ for which a C and a G_Δ achieve the performance $\bar{\sigma}(VT(G_\Delta,C)W) < \gamma$ is given by*

$$S_\Delta = S_{centre}+\Delta_S \quad ,\quad |W_S^{-1}\Delta_S| \le 1, \qquad (19)$$

with

$$S_{centre} = \frac{|V_1|^2}{|V_1|^2 + |V_2|^2 |C|^2}$$

$$|W_S|^2 = \frac{|C|^2\gamma^2}{\left(|V_1|^2+|V_2|^2|C|^2\right)\left(|W_2|^2+|W_1|^2|C|^2\right)} - \frac{|V_1|^2|V_2|^2|C|^2}{\left(|V_1|^2+|V_2|^2|C|^2\right)^2}$$

$$= \frac{|C|^2}{\left(|V_1|^2+|V_2|^2|C|^2\right)^2}\left(\frac{\left(|V_1|^2+|V_2|^2|C|^2\right)\gamma^2}{\left(|W_2|^2+|W_1|^2|C|^2\right)} - |V_1|^2|V_2|^2\right).$$

Proof With Lemma 1 it follows that all sensitivity functions S_Δ satisfying $\bar{\sigma}(VT(G_\Delta,C)W)^2 < \gamma^2$ are described by

$$\left(\left(S_\Delta - \frac{|V_1|^2}{\left(|V_1|^2+|V_2|^2|C|^2\right)}\right)\left(S_\Delta - \frac{|V_1|^2}{\left(|V_1|^2+|V_2|^2|C|^2\right)}\right)^* + \frac{|V_1|^2|V_2|^2|C|^2}{\left(|V_1|^2+|V_2|^2|C|^2\right)^2}\right)\frac{\left(|V_1|^2+|V_2|^2|C|^2\right)\left(|W_2|^2+|W_1|^2|C|^2\right)}{|C|^2} < \gamma^2,$$

which directly leads to (19). □

Using the fact that $G_\Delta = \frac{1-S_\Delta}{CS_\Delta}$, all plants achieving $\bar{\sigma}(VT(G_\Delta,C)W) < \gamma$ with C must have their frequency responses in the region described by the following corollary.

Corollary 4 *All plants G_Δ achieving $\bar{\sigma}(VT(G_\Delta,C)W) < \gamma$ are characterized by*

$$G_\Delta = \frac{D_c|V_2|^2|C|^2 + D_c\Delta}{N_c|V_1|^2 - N_c\Delta}, \text{ with } |\Delta| \le W_Y \text{ and}$$

$$W_Y = |C|\sqrt{\left(\frac{\left(|V_1|^2+|V_2|^2|C|^2\right)\gamma^2}{\left(|W_2|^2+|W_1|^2|C|^2\right)} - |V_1|^2|V_2|^2\right)}$$

Due to the LFT structure, this set can also be described in an additive structure using Proposition 1,

$$G_\Delta = G_{centre} + \Delta_a \quad , \quad \left|W_a^{-1}\Delta_a\right| \le 1$$

$$G_{centre} = C^{-1}\frac{|W_Y|^2 + |V_2|^2|C|^2|V_1|^2}{|V_1|^4 - |W_Y|^2}$$

$$W_a = C^{-1}\frac{|V_2|^2|C|^2 + |V_1|^2}{|V_1|^4 - |W_Y|^2}W_Y.$$

Note again that the set equals the exterior of the circle in case $|V_1|^4 < |W_Y|^2$.

Proof See appendix. □

Given a controller C and weighting functions V and W the corollary describes the set of all plants achieving the performance measure $\bar{\sigma}(VT(G_\Delta,C)W) < \gamma$. This set turns out to be circular at each frequency and is independent of a particular uncertainty structure and determined by C,V,W and γ only. When γ increases, indicating the allowance of a larger performance cost, this set of plants naturally becomes larger (W_Y increases). But note that the set increases with γ in a particular direction. By comparison with the dual Youla uncertainty set and its depiction in Figure 5.b note that the centre of the (circular) set always moves along the line between $\frac{|V_2|^2}{|V_1|^2}C^*$ and $-C^{-1}$, starting from $\frac{|V_2|^2}{|V_1|^2}C^*$ (for γ corresponding to $W_Y = 0$) and moving away from $-C^{-1}$. This is illustrated in Figure 9. At $|W_Y|^2 = |V_1|^4$, the centre passes through infinity after which it continues to move alone the line through $\frac{|V_2|^2}{|V_1|^2}C^*$ and $-C^{-1}$ now towards $-C^{-1}$. In this case, the set is given by the exterior of the boundary circle whose radius is now seen to decrease with increasing performance cost γ.

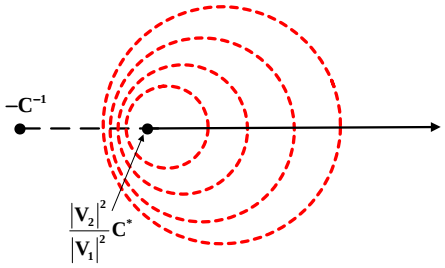

Fig. 9. Illustration of the sets of plant models that achieve a certain performance cost $J(G_\Delta,C) < \gamma$ for increasing values of γ. For increasing γ the circular set expands with its centre moving along the line through $\frac{|V_2|^2}{|V_1|^2}C^*$ and $-C^{-1}$, starting from $\frac{|V_2|^2}{|V_1|^2}C^*$ and moving away from $-C^{-1}$.

The set of Corollary 4 offers an alternative interpretation of the worst-case performance of a particular uncertainty set G. The worst-case performance over an uncertainty set G is determined by the smallest possible value of γ for which the set of Corollary 4 is just large enough to contain all the members G_Δ of the set G. It is clear that when the uncertainty in G increases, the worst-case performance (the required γ) increases. But, Corollary 4 reveals that also the positioning of the uncertainty set G with respect to $-C^{-1}$ is of crucial importance, since the set of Corollary 4 is bound to increases with γ along a particular line. Figure 10 illustrates an example in which a larger uncertainty region still leads to a smaller worst-case performance as a result of this dependence of the positioning of the uncertainty region with respect to $-C^{-1}$. The figure illustrates an identified uncertainty region (grey region) and two possible embedding regions (top and bottom dashed circles). While the embedding region in the top figure is much smaller than the embedding region in the bottom figure, the resulting worst-case performance is smaller for the larger uncertainty. This results from a more conducive positioning with respect to $-C^{-1}$. As another extreme example, Corollary 4 reveals that a certain nominal performance with G_x is achieved by many a plant G_Δ. The set of all these plants (with G_x on the boundary) could be taken as an uncertainty around G_x for free, i.e.

without changing the worst-case performance.

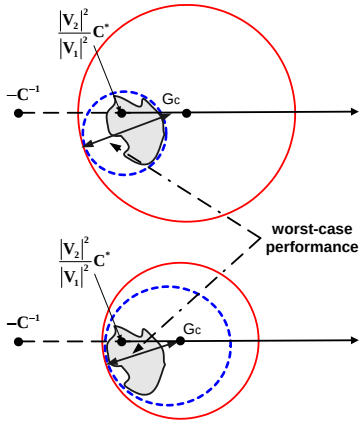

Fig. 10. Embedding an uncertainty region and the effect on the worst-case performance. The worst-case performance at a particular frequency is determined by that γ for which the set of Corollary 4 (red solid circle) is just large enough to contain the embedding set G (blue dashed-dotted circle). Therefore, the positioning of the uncertainty set with respect to $C^{-1}$is of crucial importance. Here a more conservative embedding (bottom) still leads to a better worst-case performance due to a more conducive orientation of the embedding set.

The centre of the set of plants performing robustly with the controller C lies along a line through $-C^{-1}$ and moves away from this point for increasing performance costs. This indicates a direction in which the performance cost is most sensitive to an increase in uncertainty. In other words, the closer a plant uncertainty set comes to $-C^{-1}$, the higher the performance cost. The Youla parametrization was shown to expand away from the negative inverse of the auxiliary controller C_{aux} used in the parametrization itself along a line through the nominal model G_x and $-C^{-1}$ (cf. Corr. 1). In case the auxiliary controller C_{aux} is close to the controller C to be evaluated, the Youla parameter uncertainty is 'pushed' in the right direction, i.e. in the direction being least sensitive to an increase in the worst-case performance. A further exploration of this result is beyond the scope of the current paper. Another interesting topic of research is the connection between this corollary and the results of [15] where the set of all plants/controllers achieving a certain performance with a particular controller/plant is described based on computational techniques which do include robust stability.

6.4 Identification and robust performance analysis

From the equivalence of the uncertainty structures and the fact that the boundary of the circular region at each frequency is reached for at least on member of the uncertainty set (Propositions 4 and 5), it is clear that robust performance analysis is independent of the particular structure of the uncertainty. That is, robust performance analysis can be done without conservatism on the basis of the union of circles in the frequency domain. In other words, robust performance analysis is with respect to the set of frequency responses and not with respect to a particular nominal model and uncertainty structure. System identification for control should therefore be directed towards the identification of the smallest possible plant uncertainty set rather than towards identifying a low-order nominal model and (over)bounding its uncertainty. Secondly, experiment design should be directed towards achieving this smallest uncertainty at the most relevant frequencies. Even if a low order model is required for controller design, the controller validation (robust performance analysis) should be based on the smallest possible uncertainty set that identification can provide based on the available measurement data.

In the previous sections it was shown that the worst-case performance of a controller with a (circular) plant uncertainty set can be calculated analytically. An application hereof in system identification for control is in the design of appropriate identification experiments to decrease the worst-case performance cost at a particular frequency. The analytical expressions for the worst-case performance explicitly give the amount of additional power required at each frequency to reduce the performance cost. Note, however, that the new experiment will generally also yield a new nominal model and associated controller. Related experiment design approaches for identification are elaborated in [24,20,3].

Section 6.3 gives a motivation for system identification in the dual Youla structure. The uncertainty region resulting from identification of the Youla parameter will be such that it induces a small worst-case performance cost for all controllers close to the present controller.

7 Robust performance synthesis

The final goal in identification for control is *designing* a controller achieving a certain worst-case performance over a set of plants. For SISO systems with a one-dimensional uncertainty block, this problem can be solved quite well with standard μ-synthesis (DK-iteration or LMI) [35]. However, such computational methods do not lend themselves for understanding the influence of uncertainty (structures) on the attainable performance of such methods. Fortunately, for the ν-gap uncertainty structure an analytical expression exists for a particular loop-shaped performance measure, given by $\bar{\sigma}\left(T(WG_\Delta, W^{-1}C)\right)$ [26].

Proposition 6 *[34]. Let there be a ν-gap set $G_\nu(G_x, W_v)$ as defined in (3). Consider the so-called loop-shaped performance measure $\bar{\sigma}\left(T(WG_\Delta, W^{-1}C)\right)$. Then*

$$\max_{G_\Delta \in G_\nu(G_x,W_v)} \bar{\sigma}\left(T(WG_\Delta, W^{-1}C)\right) \tag{20}$$
$$= \sin\left(arc\sin\left(\bar{\sigma}\left(T(WG_x, W^{-1}C)\right)^{-1} - arc\sin\left(W_v\right)\right)^{-1}.$$

The proposition allows for a robust performance analysis, but more importantly for a robust performance synthesis

as well. It expresses the worst-case performance of a controller C with a ν-gap set $G_\nu(G_x,W_\nu)$ in terms of the performance of C with the nominal model G_x and the chordal distance W_ν. The proposition is special since expression (20) is such that minimization of the worst-case performance $\max_{G_\Delta\in G_\nu(G_x,W_\nu)}\bar{\sigma}\left(T(WG_\Delta,W^{-1}C)\right)$ over the controller C is achieved by minimization of the nominal performance $\bar{\sigma}\left(T(WG_x,W^{-1}C\right)$ over C. In other words, the performance of G_x as a function of C has the same minimizing argument as the performance of the ν-gap set $G_\nu(G_x,W_\nu)$ as a function of C. That is, for the particular choice of uncertainty structure and performance measure it holds that

$$\arg\min_C \sup_{G_\Delta\in G} J(G_\Delta,C) = \arg\min_C J(G_x,C).$$

This expression reflects a special property of a particular combination of uncertainty structure and performance measure in the context of robust performance synthesis. This property holds also for an additive and multiplicative uncertainty structure in combination with the controller times sensitivity function $C/(1+CG_\Delta)$ as performance measure and for the inverse multiplicative uncertainty structure in combination with the plant times sensitivity function $G_\Delta/(1+CG_\Delta)$ as performance measure (for details see [11]).

Since for nominal performance optimization many techniques are available [15,26,35], robust performance optimization of a ν-gap set with the loop-shaped performance measure is straightforward.

The analysis in the previous sections shows that this result can be generalized to other uncertainty structures. Because of the fact that any of the considered uncertainty sets can be equivalently described in a ν-gap structure, Proposition 6 can be applied to the other structures as well. In the following lemma an additive structure is described in terms of an ν-gap structure.

Lemma 2 *An additive uncertainty set $G_a(G_a,W_a)$ is alternatively described in terms of a ν-gap uncertainty $G_\nu(G_\nu,W_\nu)$ with*

$$G_\nu = aG_a, \qquad |W_\nu|^2 = \frac{1}{\left(\frac{a^2}{(1-a)^2}|W_a|^2+1\right)},$$

with $a\in\mathbb{R}$ satisfying

$$a^2|G_a|^2 + a\left(1-|G_a|^2+|W_a|^2\right)-1=0. \qquad (21)$$

There are two solutions. The solutions yield sets given by the exterior and the interior of the boundary, respectively.

Proof See appendix. □

On combining Lemma 2 and Proposition 1 all (circular) uncertainty structures can be transformed into a ν-gap uncertainty description. This in turn allows for the application of Proposition 6. While the proposition can be applied directly for robust performance analysis purposes, in robust performance synthesis care has to be taken of robust stability. That is, while the worst-case performance as a function of C is to be optimized for the ν-gap nominal model G_ν of Lemma 2, the controller C will have to stabilize the original nominal model G_a.

The loop-shaping performance cost considered in Proposition 6 is not as general as the general function in (4). For more general weighting functions V and W, we have to resort to the dual form of Corollary 4. That is, for a particular plant G_Δ the set of all controllers achieving a certain performance can explicitly be given. The intersection of all these controllers when evaluated over a set of plants G is the set of all robustly performing controllers for that set. Figure 11 illustrates this interpretation of the set of robustly performing controllers at one particular frequency. For each point of an additive set $G_a(G_x,W_a)$ the (circular) set of controllers achieving a certain performance is given with Corollary 4. The intersection of these sets (thick solid circle) is the set of robustly performing controllers. The thin outer circle depicts the region of all controllers satisfying the robust stability condition $\left|\frac{C}{1+CG_x}\right| < |W_a|$, showing that this robust stability condition is automatically satisfied when using $\bar{\sigma}(VT(G_\Delta,C)W)$ as performance measure. The union of such intersections over frequency contains the frequency responses of all robustly performing controllers.

This interpretation could find a practical application as well. Given an identified uncertainty region (ellipsoidal, boxed or a set of multiple measurements of a nonparametric identification experiment), one could consider not to embed this region in a particular uncertainty structure, in terms of fitting a nominal plant and constructing an uncertainty region. Instead, given an a priori specified performance measure, the identified uncertainty could be transformed directly with Corollary 4 into a frequency domain region in which the frequency response of robustly performing controllers has to be contained. Then a controller could be 'identified' by fitting a model into this region of frequency responses. Such an approach has close connections to the Quantitative Feedback Theory approach of [22,23] and the Virtual Reference Feedback Tuning of [4]. In the latter approach, plant input and output data are mapped with an a priori performance function into "controller input and output data", i.e. data from which a controller can be identified satisfying the required performance. The approach described here is quite similar, though formulated in the frequency domain and incorporating robustness issues by starting from a model uncertainty instead of one realization of plant input and output data. In the QFT method (logarithmic) frequency domain regions (called templates) are provided for the loop transfer function CG_x instead of for C. The results in this paper provide for exact quantitative templates for a broad class of

performance measures and uncertainty structures. The identification of a parametrized controller, given a set of regions over a frequency grid, could be done by using a nonlinear optimization procedure or simply by using the engineering method of trial and error based on the visual information provided by the bode or nyquist plot.

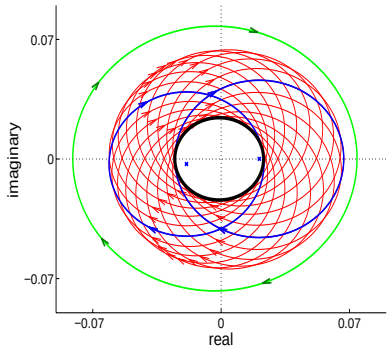

Fig. 11. Depiction at one frequency of the set of frequency responses of robustly performing controllers. For each point of an additive set $G_a(G_x, W_a)$ the (circular) set of controllers achieving a certain performance is given with Corollary 4. The intersection of these sets (thick solid circle) is the set of robustly performing controllers. The thin outer circle depicts the region of all controllers satisfying the robust stability condition $\left|\frac{C}{1+CG_x}\right| < |W_a|$.

8 Conclusions

The choice for particular uncertainty structures in identification for robust control has been analyzed for general frequency dependent performance functions. An amplitude-bounded (circular) uncertainty set following from system identification can equivalently be described in terms of an additive, Youla parameter and ν-gap uncertainty. However the equivalence is only valid when allowing nominal models and weighting functions to vary, pointing towards a desired identification setup that identifies model uncertainty sets, rather than bounding the model uncertainty around a prefixed nominal model. Closed-loop performance functions based on the uncertainty sets are again bounded by circles in the frequency domain, allowing for analytical expressions for worst-case performance evaluation, and for the evaluation of the consequences of uncertainty for robust control design. These results can be used to tune optimal experimental conditions in view of robust design. The results are a step in ongoing research towards procedures for optimal experiment-based robust control design.

Acknowledgement

Fruitful discussions with Raymond de Callafon and Xavier Bombois are gratefully acknowledged.

References

[1] P. Albertos and V. Sala, editors. *Iterative Identification and Control*. Springer-Verlag, London, UK, 2002.

[2] X. Bombois, M. Gevers, G. Scorletti, and B.D.O. Anderson. Robustness analysis tools for an uncertainty set obtained by prediction error identification. *Automatica*, 37:1629–1636, 2001.

[3] X. Bombois, G. Scorletti, M. Gevers, R. Hildebrand, and P. Van den Hof. Least costly identification experiment for control. *Submitted to Automatica. Preliminary version presented at the CDC-2004*, 2004.

[4] M.C. Campi, A. Lecchini, and S.M. Savaresi. Virtual reference feedback tuning: a direct method for the design of feedback controllers. *Automatica*, 38(8):1337–1346, 2002.

[5] J. Chen and G. Gu. *Control Oriented System Identification*. Wiley Interscience, 2000.

[6] R.A. De Callafon. *Feedback Oriented Identification for Enhanced and Robust Control*. PhD thesis, Mechan. Engin. Systems and Control Group, Delft Univ. Technology, 1998.

[7] R.A. de Callafon and P.M.J. Van den Hof. Suboptimal feedback control by a scheme of iterative identification and control design. *Mathem. Modelling of Systems*, 3(1):77–101, 1997.

[8] R.A. De Callafon and P.M.J. Van den Hof. Multivariable feedback relevant system identification of a wafer stepper system. *IEEE Trans. Control Systems Techn.*, 9(2):381–390, 2001.

[9] D.K. de Vries and P.M.J. Van den Hof. Quantification of uncertainty in transfer function estimation: a mixed probabilistic – worst-case approach. *Automatica*, 31(4):543–557, 1995.

[10] J.G.M. Dötsch. *Identification for Control Design with Application to a Compact Disk Mechanism*. PhD thesis, Mechan. Engin. Systems and Control Group, Delft Univ. Technology, 1998.

[11] S.G. Douma. *From data to robust control. System identification uncertainty and robust control design*. PhD thesis, Delft Center for Systems and Control, Delft Univ. Technology, 2005.

[12] S.G. Douma, P.M.J. Van den Hof, and O.H. Bosgra. Controller tuning freedom under plant identification uncertainty: double youla beats gap in robust stability. *Automatica*, 39(2):325–333, 2003.

[13] M. Gevers. Towards a joint design of identification and control. In H.L. Trentelman and J.C. Willems, editors, *Essays on Control: Perspectives in the Theory and its Applications*, pages 111–115. Birkhäuser, Boston, 1993.

[14] M. Gevers, X. Bombois, B. Codrons, G. Scorletti, and B.D.O. Anderson. Model validation for control and controller validation in a prediction error identification framework. *Automatica*, 39(3):403–428, 2003.

[15] K. Glover and J.C. Doyle. State space formulae for all stabilizing controllers that satisfy an H_∞-norm bound and relations to risk sensitivity. *Systems and Control Letters*, 11:167–172, 1988.

[16] G.C. Goodwin, M. Gevers, and B.M. Ninness. Quantifying the error in estimated transfer functions with application to model order selection. *IEEE Trans. Autom. Control*, 37:913–928, 1992.

[17] R.G. Hakvoort. A linear programming approach to the identification of frequency domain error bounds. In *Prepr. 10th IFAC Symp. System Identification*, volume 2, pages 195–200, 1994.

[18] R.G. Hakvoort and P.M.J. Van den Hof. Identification of probabilistic uncertainty regions by explicit evaluation of bias and variance errors. *IEEE Trans. Automatic Control*, 42(11), 1997.

[19] W.P. Heath. Bias of indirect non-parametric transfer function estimates for plants in closed loop. *Automatica*, 37:1529–1540, 2001.

[20] R. Hildebrand and M. Gevers. Identification for control: optimal input design with respect to a worst-case ν-gap cost function. *SIAM J. Control and Optimiz.*, 41(5):1586–1608, 2003.

[21] H. Hjalmarsson. From experiments to closed-loop control. *Automatica*, 41(3), 2005.

[22] I. Horowitz. *Synthesis of Feedback Systems*. Academic Press, New York, USA, 1963.

[23] I. Horowitz. Survey of quantitative feedback theory (QFT). *International Journal of Control*, 53(2):255–291, 1991.

[24] K. Lindqvist and H.Hjalmarsson. Identification for control: adaptive input design using convex optimization. In *40th IEEE Conf. Decision and Control*, Orlando, Florida, USA, 12 2001. IEEE.

[25] L. Ljung. *System Identification: Theory for the User*. Prentice-Hall, Englewood Cliffs, New Jersey, USA, 1987.

[26] D. McFarlane and K. Glover. A loop shaping design procedure using H_∞ synthesis. *IEEE Trans. Automatic Control*, 37:759–769, 1992.

[27] M. Milanese, J. Norton, H. Piet-Lahanier, and E. Walter, editors. *Bounding Approaches to System Identification*. Plenum Press, New York, 1996.

[28] M. Milanese and M. Taragna. Optimality, approximation, and complexity in set membership H_∞ identification. *IEEE Trans. Automatic Control*, 47(10):1682–1690, 2002.

[29] T.T. Tay, J.B. Moore, and R. Horowitz. Indirect adaptive techniques for fixed controller performance enhancement. *Int. J. Control*, 50(5):1941–1959, 1989.

[30] P.M.J. Van den Hof. Closed-loop issues in system identification. *Annual Reviews in Control*, 22:173–186, 1998.

[31] P.M.J. Van den Hof and R.J.P. Schrama. Identification and control–closed loop issues. *Automatica*, 31(12):1751–1770, 1995.

[32] P.M.J. Van den Hof, R.J.P. Schrama, and P.M.M. Bongers. On nominal models, model uncertainty and iterative methods in identification and control design. In R.S. Smith and M.A. Dahleh, editors, *The Modeling of Uncertainty in Control Systems*, volume 192 of *Lecture Notes in Control and Information Sciences*, pages 39–50. Springer Verlag, 1994.

[33] M. Vidyasagar. *Control System Synthesis: A Factorization Approach*. MIT Press, Cambridge, Massachusetts, USA, 1985.

[34] G. Vinnicombe. *Uncertainty and Feedback : H_∞ Loop-shaping and the ν-gap Metric*. Imperial College Press, London, UK, 2001.

[35] K. Zhou, J.C. Doyle, and K. Glover. *Robust and Optimal Control*. Prentice-Hall, New Jersey, USA, 1996.

A Proofs

Proof of Corollary 1 The Youla parametrization of (2) is rewritten as

$$\begin{aligned} G_\Delta &= \frac{\bar{N}_x + \bar{D}_c\Delta_G}{D_x - N_c\Delta_G} = \frac{\bar{N}_x\bar{D}_x - \bar{N}_x\bar{N}_c\Delta_G + \bar{D}_x\bar{D}_c\Delta_G + \bar{N}_x\bar{N}_c\Delta_G}{D_x\left(D_x - N_c\Delta_G\right)} \\ &= \frac{\bar{N}_x}{D_x} + \frac{\left(\bar{D}_c + \frac{\bar{N}_x}{D_x}\bar{N}_c\right)\Delta_G}{\left(D_x - N_c\Delta_G\right)} \\ &= \frac{\bar{N}_x}{D_x} + \frac{\left(\frac{\bar{D}_c}{N_c} + \frac{\bar{N}_x}{D_x}\right)\left(\frac{\bar{N}_c}{D_x}\Delta_G\right)}{\left(1 - \left(\frac{\bar{N}_c}{D_x}\Delta_G\right)\right)}, \end{aligned}$$

after which Proposition 1 can be applied directly, with $P_{11} = -1$, $P_{12} = \left(\frac{\bar{D}_c}{N_c} + \frac{\bar{N}_x}{D_x}\right)$, $P_{21} = 1$, $P_{22} = \frac{\bar{N}_x}{D_x}$ and $\bar{W}_Y = \frac{\bar{N}_c Q_c}{D_x Q} W_Y$.

Application of Proposition 1 leads to

$$\begin{aligned} G_{centre} &= \frac{\bar{N}_x}{D_x} + \frac{\left(\frac{\bar{D}_c}{N_c} + \frac{\bar{N}_x}{D_x}\right)\left|\bar{W}_Y\right|^2}{1 - \left|\bar{W}_Y\right|^2} \\ &= G_x\left(1 + \frac{\left|\bar{W}_Y\right|^2}{1 - \left|\bar{W}_Y\right|^2}\right) + C^{-1}\frac{\left|\bar{W}_Y\right|^2}{1 - \left|\bar{W}_Y\right|^2} \end{aligned}$$

and

$$W_a = \frac{\left(\frac{\bar{D}_c}{N_c} + \frac{\bar{N}_x}{D_x}\right)\bar{W}_Y}{1 - \left|\bar{W}_Y\right|^2} = \frac{\left(C^{-1} + G_x\right)\bar{W}_Y}{1 - \left|\bar{W}_Y\right|^2}.$$

□

Proof of Proposition 3 Proposition 2 represents $G_\nu(G_x, W_\nu)$ in terms of a dual Youla type of representation with G_x^* as nominal controller. The proof therefore can follow that of Corollary 1. However, for brevity here a proof is provided that is independent of the result of Proposition 2. All plants achieving a chordal distance $\kappa(G_\Delta(i\omega), G_x(i\omega)) \leq W_\nu$ by definition satisfy

$$\frac{\left|G_x(i\omega) - G_\Delta(i\omega)\right|^2}{\left(1 + \left|G_\Delta(i\omega)\right|^2\right)\left(1 + \left|G_x(i\omega)\right|^2\right)} \leq \left|W_\nu\right|^2$$

which can be rewritten (with omission of the argument $i\omega$ for brevity of notation) as

$$\begin{aligned} &\left|G_x - G_\Delta\right|^2 \leq \left|W_\nu\right|^2\left(1 + \left|G_\Delta\right|^2\right)\left(1 + \left|G_x\right|^2\right), \\ &\left|G_\Delta\right|^2 - G_x G_\Delta^* - G_\Delta G_x^* + \left|G_x\right|^2 \leq \\ &\qquad \left(1 + \left|G_x\right|^2\right)\left|W_\nu\right|^2 + \left|G_\Delta\right|^2\left(1 + \left|G_x\right|^2\right)\left|W_\nu\right|^2, \quad \text{or} \\ &\left|G_\Delta\right|^2\left(1 - \left(1 + \left|G_x\right|^2\right)\left|W_\nu\right|^2\right) - G_x G_\Delta^* - G_\Delta G_x^* \leq \\ &\qquad \left(1 + \left|G_x\right|^2\right)\left|W_\nu\right|^2 - \left|G_x\right|^2, \end{aligned}$$

which upon completion of the squares leads to the expression

$$\left|\left|G_\Delta\right|^2 - \frac{G_x}{\left(1 - \left(1 + \left|G_x\right|^2\right)\left|W_\nu\right|^2\right)}\right|^2 \leq \left|W_a\right|^2$$

with $|W_a|^2 =$

$$
\begin{aligned}
&= \frac{\left(1+|G_x|^2\right)|W_v|^2 - |G_x|^2}{\left(1-\left(1+|G_x|^2\right)|W_v|^2\right)} + \frac{|G_x|^2}{\left(1-\left(1+|G_x|^2\right)|W_v|^2\right)^2} \\
&= \frac{\left(1-\left(1+|G_x|^2\right)|W_v|^2 - |G_x|^2\right)\left(1+|G_x|^2\right)|W_v|^2}{\left(1-\left(1+|G_x|^2\right)|W_v|^2\right)^2} \\
&= \frac{\left(1+|G_x|^2\right)\left(1-|W_v|^2\right)\left(1+|G_x|^2\right)|W_v|^2}{\left(1-\left(1+|G_x|^2\right)|W_v|^2\right)^2},
\end{aligned}
$$

with which the corollary is proven. □

Proof of Lemma 1 For SISO plants and controllers the proof can be based on the fact that the squared maximum singular value of a rank one matrix equals the sum of squares of the elements (Frobenius norm), i.e.

$$
\begin{aligned}
&\bar{\sigma}(VT(G_\Delta, C)W)^2 \\
&= \left(|V_2|^2 + |V_1|^2 |G_\Delta|^2\right)\left|\frac{1}{1+CG_\Delta}\right|^2 \left(|W_2|^2 + |W_1|^2 |C|^2\right).
\end{aligned}
$$

Since $S_\Delta = \dfrac{1}{1+CG_\Delta}$ it holds that $G_\Delta = \dfrac{1-S_\Delta}{S_\Delta C}$ and straightforward rewriting with respect to S_Δ results in

$$
\begin{aligned}
&\bar{\sigma}(VT(G_\Delta, C)W)^2 \\
&= \left(|V_2|^2 + |V_1|^2 \left|\frac{1-S_\Delta}{S_\Delta C}\right|^2\right)|S_\Delta|^2 \left(|W_2|^2 + |W_1|^2 |C|^2\right), \\
&= \left(|V_2|^2 |S_\Delta|^2 + \tfrac{|V_1|^2}{|C|^2}|1-S_\Delta|^2\right)\left(|W_2|^2 + |W_1|^2 |C|^2\right) \\
&= \left(\left(|V_2|^2 |C|^2 + |V_1|^2\right)|S_\Delta|^2 - |V_1|^2 (S_\Delta + S_\Delta^* - 1)\right)\tfrac{|W_2|^2+|W_1|^2|C|^2}{|C|^2} \\
&= \left(|S_\Delta|^2 - \tfrac{|V_1|^2}{|V_2|^2|C^2|+|V_1|^2}(S_\Delta + S_\Delta^*) + \right. \\
&\quad \left. \tfrac{|V_1|^2}{|V_2|^2|C^2|+|V_1|^2}\right)\tfrac{\left(|V_2|^2|C^2|+|V_1|^2\right)\left(|W_2|^2+|W_1|^2|C|^2\right)}{|C|^2},
\end{aligned}
$$

which upon completion of the squares leads to expression (18). □

Proof of Corollary 4 The first part of the corollary follows from Corollary 3 and the fact that

$$
\begin{aligned}
G_\Delta &= \frac{1-S_\Delta}{S_\Delta C} = \frac{1-S_{centre}-\Delta_S}{S_{centre}C + \Delta_S C} \\
&= \frac{\left(|V_1|^2 + |V_2|^2|C|^2\right) - |V_1|^2 - \left(|V_1|^2 + |V_2|^2|C|^2\right)\Delta_S}{|V_1|^2 C + C\left(|V_1|^2 + |V_2|^2|C|^2\right)\Delta_S} \\
&= \frac{1}{C}\frac{|V_2|^2|C|^2 + \tilde{\Delta}_S}{|V_1|^2 - \tilde{\Delta}_S} \quad , \tilde{\Delta}_S = -\left(|V_1|^2 + |V_2|^2|C|^2\right)\Delta_S.
\end{aligned}
$$

The second part is obtained by application of Proposition 1. For, the above expression can be rewritten as

$$
\begin{aligned}
G_\Delta &= \frac{1}{C}\frac{|V_2|^2|C|^2 + \tilde{\Delta}_S}{|V_1|^2 - \tilde{\Delta}_S} = \frac{1}{C}\frac{\frac{|V_2|^2}{|V_1|^2}|C|^2 + \frac{1}{|V_1|^2}\tilde{\Delta}_S}{1 - \frac{1}{|V_1|^2}\tilde{\Delta}_S} \\
&= -\frac{1}{C}\frac{-\frac{|V_2|^2}{|V_1|^2}|C|^2(1 - \frac{1}{|V_1|^2}\tilde{\Delta}_S) - \left(\frac{1}{|V_1|^2} + \frac{|V_2|^2}{|V_1|^2}|C|^2\right)\tilde{\Delta}_S}{1 - \frac{1}{|V_1|^2}\tilde{\Delta}_S} \\
&= \frac{1}{C}\frac{|V_2|^2}{|V_1|^2}|C|^2 - \frac{\frac{1}{C}\frac{|V_1|^2+|V_2|^2|C|^2}{|V_1|^4}\tilde{\Delta}_S}{1 - \frac{1}{|V_1|^2}\tilde{\Delta}_S}.
\end{aligned}
$$

Therefore, with $P_{22} = \frac{1}{C}\frac{|V_2|^2}{|V_1|^2}|C|^2$, $P_{12}P_{21} = \frac{1}{C}\frac{|V_1|^2+|V_2|^2|C|^2}{|V_1|^4}$ and $P_{11} = \frac{1}{|V_1|^2}$ direct application of Proposition 1 leads to

$$
\begin{aligned}
G_{centre} &= \frac{1}{C}\frac{|V_2|^2}{|V_1|^2}|C|^2 + \frac{-\frac{1}{C}\frac{|V_1|^2+|V_2|^2|C|^2}{|V_1|^2}|W_Y|^2}{|V_1|^4 - |W_Y|^2} \\
&= \frac{1}{C}\frac{\frac{|V_2|^2}{|V_1|^2}|C|^2|V_1|^4 - \left(\frac{|V_2|^2}{|V_1|^2}|C|^2 - \frac{|V_1|^2+|V_2|^2|C|^2}{|V_1|^2}\right)|W_Y|^2}{|V_1|^4 - |W_Y|^2} \\
&= \frac{1}{C}\frac{\frac{|V_2|^2}{|V_1|^2}|C|^2|V_1|^4 + \frac{|V_1|^2}{|V_1|^2}|W_Y|^2}{|V_1|^4 - |W_Y|^2}
\end{aligned}
$$

and

$$
W_a = \frac{1}{C}\frac{\frac{|V_1|^2+|V_2|^2|C|^2}{|V_1|^4}}{1 - \frac{1}{|V_1|^4}|W_Y|^2}W_Y.
$$

□

Proof of Lemma 2 Straightforward use of Proposition 3 leads to a large, hardly tractable sequence of algebraic manipulation. A nice simplification, however, follows from the fact that G_v and W_v are completely defined by two points on the boundary circle of $G_a(G_a, W_a)$ and from the observation of Proposition 3 that

$$
G_a = \frac{G_v}{1-\left(1+|G_v|^2\right)|W_v|^2} = \frac{G_v}{a},
$$

where $a = 1-\left(1+|G_v|^2\right)|W_v|^2$,

i.e. G_v of a set $G_v(G_v, W_v)$ lies in the same direction as the centre G_a of the circle described by $G_v(G_v, W_v)$. That is, G_v should satisfy the condition

$$
\kappa(G_v, G_a\left(1+\frac{|W_a|}{|G_a|}\right)) = \kappa(G_v, G_a\left(1-\frac{|W_a|}{|G_a|}\right)) \qquad \text{(A.1)}
$$

$$
\kappa(aG_a, G_a\left(1+\frac{|W_a|}{|G_a|}\right)) = \kappa(aG_a, G_a\left(1-\frac{|W_a|}{|G_a|}\right)), \qquad \text{(A.2)}
$$

which after many but straightforward algebraic manipulations leads to condition (21). Starting from the (square of) condition (A.2) it holds that,

$$\frac{\left|a-(1+\frac{|W_a|}{|G_a|})\right|^2|G_a|^2}{\left(1+\left|G_a(1+\frac{|W_a|}{|G_a|})\right|^2\right)\left(1+|aG_a|^2\right)}=\frac{\left|a-(1-\frac{|W_a|}{|G_a|})\right|^2|G_a|^2}{\left(1+\left|G_a(1-\frac{|W_a|}{|G_a|})\right|^2\right)\left(1+|aG_a|^2\right)}$$
$$=\frac{a^2-2a(1+\frac{|W_a|}{|G_a|})+(1+\frac{|W_a|}{|G_a|})^2}{1+|G_a|^2\left(1+\frac{|W_a|}{|G_a|}\right)^2}=\frac{a^2-2a(1-\frac{|W_a|}{|G_a|})+(1-\frac{|W_a|}{|G_a|})^2}{1+|G_a|^2\left(1-\frac{|W_a|}{|G_a|}\right)^2}$$
$$=\frac{a^2-2a-2a\frac{|W_a|}{|G_a|}+1+2\frac{|W_a|}{|G_a|}+\frac{|W_a|^2}{|G_a|^2}}{1+|G_a|^2\left(1+2\frac{|W_a|}{|G_a|}+\frac{|W_a|^2}{|G_a|^2}\right)}=\frac{a^2-2a+2a\frac{|W_a|}{|G_a|}+1-2\frac{|W_a|}{|G_a|}+\frac{|W_a|^2}{|G_a|^2}}{1+|G_a|^2\left(1-2\frac{|W_a|}{|G_a|}+\frac{|W_a|^2}{|G_a|^2}\right)}$$
$$=\frac{\left(a^2-2a+1+\frac{|W_a|^2}{|G_a|^2}\right)+2\frac{|W_a|}{|G_a|}(1-a)}{1+|G_a|^2\left(1+\frac{|W_a|^2}{|G_a|^2}\right)+2|G_a||W_a|}=\frac{\left(a^2-2a+1+\frac{|W_a|^2}{|G_a|^2}\right)-2\frac{|W_a|}{|G_a|}(1-a)}{1+|G_a|^2\left(1+\frac{|W_a|^2}{|G_a|^2}\right)-2|G_a||W_a|}.$$

Now, for general numbers a,b,c,d it holds that the equation $\frac{a+b}{c+d}=\frac{a-b}{c-d}$ implies $bc=ad$. Therefore we have that

$$2\frac{|W_a|}{|G_a|}(1-a)\left(1+|G_a|^2\left(1+\frac{|W_a|^2}{|G_a|^2}\right)\right)$$
$$=\left(a^2-2a+1+\frac{|W_a|^2}{|G_a|^2}\right)2|G_a||W_a|,\quad\text{or}$$
$$(1-a)\left(1+|G_a|^2\left(1+\frac{|W_a|^2}{|G_a|^2}\right)\right)$$
$$=\left(a^2-2a+1+\frac{|W_a|^2}{|G_a|^2}\right)|G_a|^2,\quad\text{leading to}$$
$$1-a\left(1+|G_a|^2\left(1+\frac{|W_a|^2}{|G_a|^2}\right)\right)=\left(a^2-2a\right)|G_a|^2$$
$$a^2|G_a|^2+a\left(1+|W_a|^2-|G_a|^2\right)-1=0.$$

Then the rest is simple since

$$G_a=\frac{G_\nu}{1-\left(1+|G_\nu|^2\right)|W_\nu|^2}=\frac{G_\nu}{a}$$
$$W_a=\frac{\sqrt{\left(1-|W_\nu|^2\right)}\left(|G_\nu|^2+1\right)|W_\nu|}{a},$$

of which the last equation leads to Lemma 2 in a straightforward manner using the fact that

$$a=1-\left(1+|G_\nu|^2\right)|W_\nu|^2$$
$$\left(1+|G_\nu|^2\right)=\frac{1-a}{|W_\nu|^2},$$

and taking the expression of W_a

$$a^2|W_a|^2=\left(1-|W_\nu|^2\right)\left(|G_\nu|^2+1\right)^2|W_\nu|^2$$
$$a^2|W_a|^2=\left(1-|W_\nu|^2\right)\left(\frac{1-a}{|W_\nu|^2}\right)^2|W_\nu|^2$$
$$a^2|W_a|^2|W_\nu|^2=(1-a)^2-(1-a)^2|W_\nu|^2$$
$$|W_\nu|^2=\frac{(1-a)^2}{\left(a^2|W_a|^2+(1-a)^2\right)}$$
$$|W_\nu|^2=\frac{1}{\left(\frac{a^2}{(1-a)^2}|W_a|^2+1\right)},$$

which concludes the proof.

□